

## Editor's Choice

***Salmonella* methylglyoxal detoxification by STM3117-encoded lactoylglutathione lyase affects virulence in coordination with *Salmonella* pathogenicity island 2 and phagosomal acidification**

Sangeeta Chakraborty, Debalina Chaudhuri, Arjun Balakrishnan and Dipshikha Chakravorty

Department of Microbiology and Cell Biology, Indian Institute of Science, Bangalore, India

## Correspondence

Dipshikha Chakravorty  
dipa@mcbli.iisc.ernet.in

Intracellular pathogens such as *Salmonella enterica* serovar Typhimurium (*S. Typhimurium*) manipulate their host cells through the interplay of various virulence factors. A multitude of such virulence factors are encoded on the genome of *S. Typhimurium* and are usually organized in pathogenicity islands. The virulence-associated genomic stretch of *STM3117–3120* has structural features of pathogenicity islands and is present exclusively in non-typhoidal serovars of *Salmonella*. It encodes metabolic enzymes predicted to be involved in methylglyoxal metabolism. *STM3117*-encoded lactoylglutathione lyase significantly impacts the proliferation of intracellular *Salmonella*. The deletion mutant of *STM3117* ( $\Delta$ *lgl*) fails to grow in epithelial cells but hyper-replicates in macrophages. This difference in proliferation outcome was the consequence of failure to detoxify methylglyoxal by  $\Delta$ *lgl*, which was also reflected in the form of oxidative DNA damage and upregulation of *kefB* in the mutant. Within macrophages, the toxicity of methylglyoxal adducts elicits the potassium efflux channel (KefB) in the mutant which subsequently modulates the acidification of mutant-containing vacuoles (MCVs). The perturbation in the pH of the MCV milieu and bacterial cytosol enhances the *Salmonella* pathogenicity island 2 translocation in  $\Delta$ *lgl*, increasing its net growth within macrophages. In epithelial cells, however, the maturation of  $\Delta$ *lgl*-containing vacuoles were affected as these non-phagocytic cells maintain less acidic vacuoles compared to those in macrophages. Remarkably, ectopic expression of Toll-like receptors 2 and 4 on epithelial cells partially restored the survival of  $\Delta$ *lgl*. This study identified a novel metabolic enzyme in *S. Typhimurium* whose activity during intracellular infection within a given host cell type differentially affected the virulence of the bacteria.

Received 13 March 2014

Accepted 20 June 2014

**INTRODUCTION**

The genus *Salmonella* comprises facultative intracellular pathogens (Haraga *et al.*, 2008) notorious for causing persistent gastrointestinal infections in a number of hosts that often lead to fatal systemic diseases (Jantsch *et al.*, 2011). The intracellular life of the pathogen exists within a phagosomal/endosomal vacuole called a *Salmonella*-containing vacuole (SCV) (Dandekar *et al.*, 2012) whose maturation dynamics are similar to those of the canonical endocytic

pathway and are modulated by several bacterial virulence factors (Drecktrah *et al.*, 2008; Jantsch *et al.*, 2011). Typically, combinations of virulence factors are employed to combat the attack mounted by the host. For instance, metabolic and detoxifying enzymes are utilized for rigorous adaptation in nutrient-limiting conditions and exploitation of host resources, thereby favouring pathogen persistence.

Metabolism of *Salmonella enterica* serovar Typhimurium (*S. Typhimurium*) is remarkably different in epithelial cells and macrophages due to modulation in the expression of key metabolic enzymes in the two host cell types (Eisenreich *et al.*, 2010). Pathogens generally adapt themselves as per their host cell milieu and their metabolic enzymes play a pivotal role in this adaptation process. Pathogens such as *S. Typhimurium*, *Shigella flexneri*, *Mycobacterium tuberculosis* and *Listeria monocytogenes* utilize different substrates, e.g. glucose, C<sub>3</sub> compounds, C<sub>2</sub> units and glycerol, respectively (Eisenreich *et al.*, 2010). Pathogen-specific metabolic adaptations subsequently activate those virulence factors in the

**Abbreviations:** AMP, antimicrobial peptide; BAF, bafilomycin A1; BMDM, bone-marrow-derived macrophage; DiBAC<sub>4</sub>(3), bis-(1,3-dibutylbarbituric acid)-trimethine oxonol; EEA1, early endosome autoantigen 1; HBD, human  $\beta$ -defensin; LAMP1, lysosome-associated membrane protein 1; MCV, mutant-containing vacuole; PCA, perchloric acid; p.i., post-infection; q, quantitative; RT, real-time; SCV, *Salmonella*-containing vacuole; SPI, *Salmonella* pathogenicity island; TLR, Toll-like receptor; TTSS, type III secretion system.

Five supplementary figures are available with the online version of this paper.

pathogen which are required for its intracellular lifestyle. Intracellular *Salmonella* within epithelial cells and macrophages uses glucose as the preferred carbon source, and mutants defective in glycolysis or glucose uptake are impaired in their replication capacity. However, in situations of limited glycolytic carbon sources, e.g. *in vivo* infections, survival of *S. Typhimurium* is strongly dependent on the acquisition of anabolic monomers such as purines and amino acids from the host cell into the SCVs (Fields *et al.*, 1986; Mercado-Lubo *et al.*, 2009). Both glycolysis and amino acid degradation have been shown to contribute to the intracellular pool of methylglyoxal (Ferguson *et al.*, 1998). Considering the dissimilar preference of metabolic pathways in different host cells, it was interesting to investigate the consequences of the methylglyoxal pathway within macrophages and epithelial cells. Currently, very little information exists on methylglyoxal catabolism in intracellular pathogens. Elevated levels of mycobacteria-induced methylglyoxal and advanced glycation end-products in granulomatous lesions have been demonstrated to induce apoptosis of the resident macrophages as well as alter immune response genes (Rachman *et al.*, 2006). The enhanced level of lactoylglutathione lyase (methylglyoxal detoxifying enzyme) has also been implicated in contributing to *Streptococcus mutans* aciduricity in dental plaques (Korithoski *et al.*, 2007). Upregulation of either bacterial methylglyoxal-detoxifying genes or level of endogenous methylglyoxal during infection implies that pathogens exploit the methylglyoxal pathway differently to persist in host environs. Glyoxalase I (lactoylglutathione lyase) and glyoxalase II are the detoxifying enzymes which are pivotal in contributing to survival against toxic effects of electrophiles such as methylglyoxal (Booth *et al.*, 2003; MacLean *et al.*, 1998; Thornalley, 2008).

Unlike other bacteria which strictly harbour single copies of each *glxI* and *glxII*, *S. Typhimurium* has two genomic loci encoding putative glyoxalase I apart from the canonical glyoxalase I gene (*glxI*) (Campos-Bermudez *et al.*, 2007; Töttemeyer *et al.*, 1998). *gloA* encodes the canonical GlxI, whilst *STM3117* and *yaeR* encode putative GlxI (Campos-Bermudez *et al.*, 2007; Eriksson *et al.*, 2003; Santiviago *et al.*, 2009; Shi *et al.*, 2006). *STM3117* (Gene ID: 1254640) shares only 24% homology with the Ni<sup>+</sup>-dependent glyoxalase I of *Escherichia coli*. Curiously, *STM3117* is part of the virulence-associated operon (*STM3117–3120*) (Haneda *et al.*, 2009) which has three downstream coding regions and was predicted to be involved in the methylglyoxal pathway (Shi *et al.*, 2006). The *STM3117–3120* operon along with a stretch of 14 downstream ORFs, clustered adjacent to the tRNA *pheV* gene, have been denoted as *Salmonella* pathogenicity island (SPI)-13 due to the characteristic low G + C content, similar to typical pathogenicity islands (Shah *et al.*, 2005). In accordance, the homologous region corresponding to *STM3117–3120* in *S. enteritidis* was observed to be crucial for survival in chicken macrophages (Shah *et al.*, 2005). In transcriptome analysis of *S. Typhimurium* from macrophages, seven- to 20-fold upregulation of the four members of the *STM3117–3120* operon was observed

(Eriksson *et al.*, 2003). Based on the abundance of proteins in infected macrophages, it was demonstrated that *STM3117* contributes to colonization within natural resistance-associated macrophage protein negative (NRAMP1<sup>-</sup>) macrophages (Shi *et al.*, 2006) and the gene was essential for survival *in vivo* (Haneda *et al.*, 2009; Santiviago *et al.*, 2009). Contrary to this, the transcriptome of *S. Typhimurium* in epithelial cells did not show any appreciable induction in the expression of *STM3117*, *STM3119* and *STM3120* during infection (Hautefort *et al.*, 2008).

It is known that defects in methylglyoxal detoxification induce expression of *kefB* (K<sup>+</sup> efflux channel) in bacterial cells (Ferguson *et al.*, 1997). The channel works by antiporting H<sup>+</sup> against a K<sup>+</sup> efflux. In this work, we show that within macrophages, absence of *STM3117* elicits *kefB* in *S. Typhimurium* which antiports H<sup>+</sup> from mutant-containing vacuoles (MCVs) into the bacterial cytosol, causing a decrease in the bacterial pH (pHBact). The relative lowering of the bacterial pH with respect to MCVs enhances SPI-2 translocon secretion, increasing the proliferation of  $\Delta$ *glI*. By employing an *STM3117*-overexpressing strain, we showed a reversal in the trend with reduced SPI-2 secretion and proliferation. In epithelial cells, additional Toll-like receptor (TLR) 2 and 4 signalling could rescue the defective proliferation and maturation of  $\Delta$ *glI* containing vacuoles. Altogether, our results offer an insight on the possibilities of varied outcomes in the intracellular survival of *S. Typhimurium* in response to the activity of *STM3117*.

## METHODS

**Bacterial strains and growth conditions.** The bacterial strains and plasmids used in this study are listed in Table 1. *S. Typhimurium* NCTC 12023 was used as the parental WT strain. Bacteria were routinely grown at 37 °C in LB medium containing appropriate antibiotics unless otherwise mentioned. Nalidixic acid, kanamycin and ampicillin were each used at 50 µg ml<sup>-1</sup>. Generation of  $\Delta$ *glI*,  $\Delta$ *kefB* and  $\Delta$ *glI*/ $\Delta$ *kefB* double-knockout strains with deletion of *STM3117*, *kefB* and both genes, respectively, was carried out using the one-step gene deletion strategy (Datsenko & Wanner, 2000; Eswarappa *et al.*, 2008). For double knockout, the second gene was replaced with a chloramphenicol resistance cassette (pKD3). The knockout primers and confirmatory primers are listed in Table 2. For methylglyoxal sensitivity, 1 × 10<sup>5</sup> exponential-phase bacteria were either exposed to 0.2 mM methylglyoxal in LB or left untreated and were plated every hour until 3 h to enumerate the number of c.f.u. surviving. Growth was calculated for both untreated and treated sets by dividing the c.f.u. ml<sup>-1</sup> at indicated time point by the c.f.u. ml<sup>-1</sup> at the initial time point. For immunoblot analyses of SPI-2 and SPI-1 secreted proteins, F-medium (Eswarappa *et al.*, 2008) and LB with 0.3 M NaCl were used, respectively. Kinetic analyses of the *STM3117* apoenzyme and holoenzyme with supplemented divalent metal ions were performed as described previously (Clugston *et al.*, 2004; Korithoski *et al.*, 2007). The method for determination of methylglyoxal in bacterial cells was adapted with modifications from Cordeiro *et al.* Briefly, 100 ml exponential-phase culture (OD<sub>600</sub> 0.5) corresponding to 0.01 g bacterial wet weight was used. Cells were deproteinized with 3 ml 5 M perchloric acid (PCA), stirred and immediately frozen in liquid nitrogen. The frozen cultures were centrifuged at 13000 g for 30 min to remove the PCA precipitate. The supernatant was used for quantification of endogenous methylglyoxal. To 800 µl supernatant, 100 µl

**Table 1.** Strains and plasmids used in this study

Background	Strain/plasmid	Description	Reference
S. Typhimurium	NCTC 12023	WT STM (Nal <sup>r</sup> )	Chakravorty <i>et al.</i> (2005)
	$\Delta lgl$	WT 12023 $\Delta lgl::Kan$ (Km <sup>r</sup> )	This study
	$\Delta lgl$ -pQE: <i>lgl</i>	$\Delta lgl$ pQE60:: <i>lgl</i>	This study
	$\Delta lgl$ -pTrc: <i>lgl</i>	$\Delta lgl$ pTrc99c:: <i>lgl</i>	This study
	$\Delta kefB$	WT 12023 $\Delta kefB::Kan$ (Km <sup>r</sup> )	This study
	$\Delta lgl/\Delta kefB$	WT 12023 $\Delta lgl::Kan::\Delta kefB::Cat$ (Km <sup>r</sup> , Chl <sup>r</sup> )	This study
Plasmid	pFPV25.1-mCherry	Amp <sup>r</sup>	Chakravorty <i>et al.</i> (2005)
	pKD4	pANT5 <sub>γ</sub> derivative (Km <sup>r</sup> )	Datsenko & Wanner (2000)
	pKD46	pBAD18 derivative (Amp <sup>r</sup> )	Datsenko & Wanner (2000)
	pHG86	7 kb, promoterless reporter plasmid carrying <i>lacZ</i> gene (Amp <sup>r</sup> )	Das <i>et al.</i> (2009)
	pTrc99c	<i>S. Typhimurium lgl</i> complementing vector (Amp <sup>r</sup> )	This study
	pQE60	3.4 kb, low-copy-number vector; containing T5 promoter, T5 transcription start site and ColE1 origin of replication (Amp <sup>r</sup> )	Das <i>et al.</i> (2009)
	pCMV1:hTLR2-FLAG	Human TLR2 without leader (N-terminal FLAG fusion) (Amp <sup>r</sup> )	Kind gift from Dr Schnare (University of Marburg, Germany)
	pCMV1:hTLR4-FLAG	Human TLR4 without leader (N-terminal FLAG fusion) (Amp <sup>r</sup> )	Kind gift from Dr Schnare (University of Marburg, Germany)
	pCMV1:mTLR2(DN)	Mouse TLR2 (dominant negative) cloned in pCMV1 (Amp <sup>r</sup> )	Kind gift from Dr Balaji (Indian Institute of Science, India)
	pCDNA3.1:mTLR4(DN)	Mouse TLR4 (dominant negative) cloned in pCDNA3.1 (Amp <sup>r</sup> )	Kind gift from Dr Schnare (University of Marburg, Germany)

7.2 mM *o*-phenylenediamine and 100  $\mu$ l 5 M PCA were added for derivatization to 2-methylquinoxaline. 5-Methylquinoxaline was added as an internal standard. The quinoxaline derivative of methylglyoxal and the internal standard 5-methylquinoxaline were analysed by a reverse-phase C18 column at 330 nm absorbance; 68 vol.% 10 mM KH<sub>2</sub>PO<sub>4</sub> (pH 2.5) and 32 vol.% HPLC-grade acetonitrile were used as the mobile phase at an isocratic flow rate of 1 ml min<sup>-1</sup>. Duplicate injections were made for each sample. The retention times of 2- and 5-methylquinoxaline were 6 and 8.75 min, respectively. A standard curve for methylglyoxal was generated by derivatizing increasing concentrations of methylglyoxal (0.2–20 nmol). The concentration of endogenous methylglyoxal was measured by calculating the peak heights of the analyte between WT and  $\Delta lgl$ , and determining their corresponding concentrations from the 2-methylquinoxaline standard curve.

**Construction of plasmids.** Low-copy-number plasmid construct pQE60: *lgl*, which expresses *STM3117* from a T5 promoter, was constructed by cloning the 435 bp *STM3117* ORF from WT 12023 strain into the *Bam*HI/*Hind*III site of pQE60 with the primers listed in Table 2. Overexpressing construct pTrc: *lgl* was generated similarly by cloning at the same restriction sites of the pTrc99c vector. The constructs were transformed into the  $\Delta lgl$  background generating  $\Delta lgl$ -pQE60: *lgl* and  $\Delta lgl$ -pTrc: *lgl* clones, respectively. For analyzing the expression of SPI-1 genes (TTSS-1), promoters (~200 bp upstream from the start site) of two SPI-1 genes, *invF* and *sicA*, were transcriptionally fused upstream of a promoterless *lacZ* in pHG86. The *lacZ* transcriptional fusions were transformed into WT and  $\Delta lgl$  strains. pFPV25.1-mCherry (Chakravorty *et al.*, 2002)-transformed *S. Typhimurium* was used for analysing the expression of intracellular SPI-2 effectors.

**Gentamicin protection assays.** RAW264.7, U937 and INT-407 cells were maintained in Dulbecco's modified Eagle's medium (DMEM) supplemented with 10% FCS. For Caco-2 cells, non-essential amino acids solution was added as a supplement. Bone-marrow-derived macrophages (BMDMs) were obtained as described previously (Das

*et al.*, 2010). Gentamicin protection assays were performed as described previously at m.o.i. 10 (Eswarappa *et al.*, 2008). The intracellular growth was determined by dividing the c.f.u. at 16 h by that at 2 h post-infection (p.i.). For epithelial cell infections, overnight culture was subcultured at 1:33 and incubated for 3 h.

For the epithelial cell invasion assay, infected cells were lysed after 1 h of gentamicin (100  $\mu$ g ml<sup>-1</sup>) treatment. The invasiveness was represented as: (no. of intracellular bacteria/no. of input bacteria)  $\times$  100.

To inhibit vacuolar acidification, bafilomycin A1 (BAF) was used at 50 nM. To enumerate the percentage of cytosolic *S. Typhimurium*, chloroquine was used at 50  $\mu$ g ml<sup>-1</sup>. Cells were pretreated with BAF for 45 min followed by gentamicin protection assay. Chloroquine was added at the desired time points p.i. and an additional 1 h was given for the compound to kill the vacuolar bacteria before lysing with 0.1% Triton X-100. The number of cytosolic bacteria was determined as the percentage of bacteria recoverable after chloroquine treatment compared with the untreated total (vacuolar and cytosolic both) bacteria.

**In vitro secretion assays and immunoblotting.** For analyses of expression of SPI-1 and SPI-2 proteins, the procedure of Ehrbar *et al.* (2003) and Hölzer & Hensel (2010) was adapted with slight modifications. Bacteria were diluted in either SPI-1-inducing medium (LB with 0.3 M NaCl) or SPI-2-inducing medium (F-medium), and incubated for 3 and 7 h, respectively. Bacteria from 1 ml culture were harvested and resuspended in SDS loading buffer according to the optical density (OD<sub>600</sub> of 1 ml of culture  $\times$  100 =  $\mu$ l sample buffer). This fraction represented the whole-cell lysate. Secreted or membrane-attached protein fractions were isolated from 10 ml cultures grown in appropriate media. For extraction of the secreted protein fraction (SipC), culture supernatant was filtered (0.2  $\mu$ m membrane filter) and proteins were precipitated overnight at 4 °C with 10% (w/v) TCA. For isolation of the surface-associated protein fraction

**Table 2.** Forward (F) and reverse (R) primers used in the study

Primer	Sequence
<b>Knockout</b>	
<i>STM3117</i> F	TAAACATACTGCGAAATTTCAATTAAGTTTCCATCAGGGTCATATGAATATCCTCCTTAG
<i>STM3117</i> R	ATGCTATTTTTAATGTAGCATCCCTAAAATATAAACATCATGAGTGTAGGCTGGAGCTGCTTC
<i>kefB</i> F	CTACTCAAATTCATCCCAGCCATCCAACCTGGCGCCGTTCCCATATGAATATCCTCCTTAG
<i>kefB</i> R	ATGGAAGGTGCTGATTTATTGACCGCGGGAGTGTGGTGTAGGCTGGAGCTGCTTC
<b>Complementation</b>	
<i>STM3117</i> F	ATCGGGATCCATGCTATTTTTTAATG
<i>STM3117</i> R	ATCGAAGCTTTTAAACATACTGC
<b>Reporter construct</b>	
<i>invF</i> (promoter) F	ATGCGAATTCCTCCATCCAGATGAC
<i>invF</i> (promoter) R	ATGCGGATCCATGCAGCTTTTGC
<i>sicA</i> (promoter) F	ATGCGAATTCGGAGAAGGTTGGCGTACCTGTG
<i>sicA</i> (promoter) R	ATGCGGATCCCTTACTCCTGTTATCTGTCACCGA
<b>qRT-PCR</b>	
<i>hilA</i> F	GCAAACCTCCCGACGATGTAT
<i>hilA</i> R	TTAACATGTCGCCAAACAGC
<i>invF</i> F	AGATCGTAAACGCTGCGAGT
<i>invF</i> R	CTGCACAAACGACGAAAATG
<i>prgH</i> F	TTCTTGCTCATCGTGTTCG
<i>prgH</i> R	GAGATACGTTGTGGGCTCGT
<i>sptP</i> F	GAGCGATGGAATGCCTGTGC
<i>sptP</i> R	ATGCACCTCGCCAAAGGTGTAGC
<i>mutM</i> F	AGCCGCTAAGCGATGAGTTT
<i>mutM</i> R	CCAGGGTTTAATCGCCGTCT
<i>mutY</i> F	ACGACAAATACGGGCGGAAA
<i>mutY</i> R	AAGGAATCACCGTCGTCACC
<i>mutT</i> F	GGAAGAGGTGGGGATTACGC
<i>mutT</i> R	CGTTCAACCAGCCAAAACCA
<i>STM3117</i> F	GGTCCCTGATGTAGATAGACATTATC
<i>STM3117</i> R	CCGATAAATGATGTTGTGTCTGAG
<i>kefB</i> F	CCAGCTTCATCGTGTCTTCCGGT
<i>kefB</i> R	CTGTCACATTATCAATGATGACCAC
<i>ssaV</i> F	ATTACATCATCGACAAATAAAATTTCTGGAGTCGCAGTGTAGGCTGGAGCTGCTTC
<i>ssaV</i> R	GGGGGCGGATATTTACAGCCTCAGACGTTGCATCAATCATATGAATATCCTCCTTAG
<i>ssaP</i> F	GAAGTCTGGGTTGCCATGC
<i>ssaP</i> R	TATGCAGCAACTGAGACTCC

(SseB and SseD), the bacterial pellet (from 10 ml culture volume) was mixed with ice-cold PBS (1 ml), vortexed vigorously for 2 min and centrifuged for 30 min at 8000 g. The rapid vortexing enabled the loosely attached surface proteins to come into the suspension. The TCA precipitates of both the supernatant fraction and the surface-attached fraction were washed with ice-cold acetone, air-dried and finally resuspended in SDS loading buffer; 50 µg total protein was loaded on 12% SDS-PAGE gels. For immunoblot analysis, affinity-purified rabbit polyclonal antibodies against *Salmonella* SipC, SseB and SseD were used. Equal protein loading for cell-associated protein fractions was determined by levels of DnaK. For secreted and surface-attached proteins, either Coomassie-blue-stained gels or culture volumes with equivalent OD<sub>600</sub> were used for equal loading.

**Immunofluorescence microscopy.** For intracellular SPI-2 expression and SCV maturation dynamics, RAW264.7 or INT-407 cells, seeded at a density of  $3 \times 10^4$  cells per coverslip, were infected with bacteria at m.o.i. 20. Infected and PFA (3%) -fixed monolayers were incubated with specific antibodies against mouse or human lysosome-associated membrane protein 1 (LAMP1) (rat anti-mouse LAMP1 and mouse anti-human LAMP1; Developmental Studies Hybridoma

Bank), EEA1 (mouse anti-EEA1 mAb; BD Biosciences), SseB (affinity-purified polyclonal rabbit antibody conjugated to FITC), SseD (polyclonal rabbit serum), SipC (polyclonal rabbit serum) and *S. Typhimurium* (anti-*Salmonella* O-antigen) as per the experiment. Images were obtained using Zeiss LSM 510 and/or 710 confocal microscopes under a  $\times 63$  oil immersion objective. Co-localization percentage of SCV membrane markers with the bacterial population was determined by pixel-to-pixel co-localization of LAMP1 or EEA1 (red) with FITC-labelled *S. Typhimurium* (green). For scoring the percentages of vacuolar and cytosolic bacteria, co-localization values  $>20\%$  (for LAMP1) were considered vacuolar and  $\leq 20\%$  were considered cytosolic. For cytosolic bacteria, the association with poly-ubiquitinated proteins (probed with FK2 poly-ubiquitinated protein mAb) was quantified.

**Mouse experiment.** BALB/c and C57BL/6 mice (6–8 weeks old) were infected either orally or intraperitoneally under aseptic conditions with  $10^6$  and  $10^3$  c.f.u. per mouse, respectively, of overnight bacterial culture. For organ infiltration studies, livers and spleens were aseptically removed, 4 days after infection. They were weighed and homogenized in 1 ml ice-cold PBS. Serial dilutions of

the homogenate were plated on LB agar with appropriate antibiotics and the c.f.u. was calculated per gram weight of organ for liver and per organ for spleen.

**Antimicrobial peptide (AMP) sensitivity assay.** Exponentially grown bacteria (obtained after 3 h of growth post 1:50 subculture) were freshly subcultured in 0.5% tryptone/0.5% sodium chloride and 10 mM potassium phosphate buffer for determining the sensitivity against protamine sulfate and human  $\beta$ -defensin (HBD) 1, respectively, as described previously (Eswarappa *et al.*, 2008). For flow-cytometric analysis, the samples (both treated and untreated) were treated with bis-(1,3-dibutylbarbituric acid)-trimethine oxonol [DiBAC<sub>4</sub>(3)] at 1  $\mu$ g ml<sup>-1</sup> for 10 min followed by FACS analysis. The weighted means for DiBAC<sub>4</sub>(3) fluorescence was calculated. For assessing the colocalization of HD5 with intracellular bacteria, INT-407 cells were infected with either mCherry-WT or mCherry- $\Delta$ *lgl*. At the specified time points, the infected monolayers were stained with affinity-purified anti-HD5 (Alpha Diagnostic International).

**$\beta$ -Galactosidase reporter assays.** Promoter activity of two SPI-1 genes, *invF* and *sicA* was assessed using transcriptional fusions to *lacZ* as described previously (Marathe *et al.*, 2010). Reporter strains were grown in SPI-1-inducing media until exponential phase and  $\beta$ -galactosidase activity was checked by measuring the absorbance of the coloured product at the end of the assay at 495 nm. Data were expressed as Miller units normalized to bacterial growth (OD<sub>600</sub>).

**Quantitative real-time (qRT)-PCR.** For analysing the transcript levels of *STM3117* expressed from pQE60 and pTrc99c, total RNA was isolated from  $\Delta$ *lgl*-pQE:*lgl* and  $\Delta$ *lgl*-pTrc:*lgl* strains. The relative expression level of *STM3117* was normalized to that from WT. For SPI-1 genes, total bacterial RNA was isolated from cultures grown under SPI-1-inducing medium for 3 h. For the expression levels of DNA repair genes, *kefB*, and SPI-2 genes *ssaP* and *ssaV* in intramacrophage *S. Typhimurium*, RNA was isolated from intracellular bacteria within RAW264.7 cells (4 h p.i) as described previously (Eriksson *et al.*, 2003). Approximately,  $2 \times 10^8$  bacteria ml<sup>-1</sup> were taken for resuspension in TRIzol (Sigma) followed by isolation of RNA as per the manufacturer's protocol. Random hexamer primers were used to generate a cDNA pool from each RNA sample. Total DNase-treated RNA (1  $\mu$ g) was reverse transcribed using BioScript Moloney murine leukaemia virus reverse transcriptase (Bioline) according to the manufacturer's protocol. qRT-PCRs were carried out using the Kapa SYBR Green RT-PCR kit (Kapa Biosystems). Specific primer pairs are listed in Table 2. They generated ~100–150 bp amplicons. Cycle threshold (C<sub>t</sub>) was measured for each reaction and the expression fold change was measured by the 2<sup>- $\Delta\Delta$ C<sub>t</sub></sup> method. Relative expression levels were normalized to 16S rRNA levels.

**Eukaryotic cells and DNA transfection.** RAW264.7 and INT-407 cells were transiently transfected with pCMV:hTLR2-FLAG and pCMV:hTLR4 constructs (kind gift from Dr Markus Schnare, University of Marburg, Germany) using polyethyleneimine. Transfected cells were examined by confocal microscopy for expression of membrane FLAG tagged human TLR2 and 4. At 48 h post-transfection, the cells were infected with WT and  $\Delta$ *lgl*, and the monolayers were fixed at the indicated time points for analysis by confocal microscopy. Untransfected RAW264.7 and INT-407 cells were also tested for expression of TLR4 by immunofluorescence. RAW264.7 cells transiently transfected with a dominant-negative mutant construct of mouse TLR2 (kind gift from Professor K. N. Balaji, Indian Institute of Science, India) and 4 (kind gift from Dr Markus Schnare) were infected similarly for analysis by confocal microscopy.

**Measurement of phagosomal pH.** Analysis of the pH of *S. Typhimurium* SCVs was performed according to a previous report (Wong *et al.*, 2011). Bacteria were either dually labelled with a

pH-sensitive probe (pHrodo, which emits red fluorescence in an acidic environment; Invitrogen) and a pH-insensitive probe Alexa Fluor 488 (green) or singly with pH-sensitive FITC as described previously (Bernardo *et al.*, 2010). The calculated fluorescence ratios of pH-sensitive and pH-insensitive probes (in the dual-labelling process) and mean fluorescence intensity (in the single-labelling process) were used to determine phagosomal pH according to a calibration curve. Phagosomal pH was measured with a FACSCanto II (BD Biosciences). pH calibration was performed by incubating infected RAW264.7 or INT-407 cells in 10 mM phosphate citrate buffer of predetermined pH (4.0–6.0) containing 20  $\mu$ M nigericin for equilibration.

## RESULTS

### *STM3117*-encoded lactoylglutathione lyase metabolizes endogenous methylglyoxal in *S. Typhimurium*

In *S. Typhimurium*, the four coding regions from *STM3117* to *STM3120* constitute an operon, and encode lactoylglutathione lyase, monoamine oxidase, acetyl-CoA hydrolase and a LysR-type transcriptional regulator, respectively (Fig. 1a) (Haneda *et al.*, 2009). Eriksson *et al.* (2003), based on the transcriptome analysis, had predicted that *STM3117* promoted methylglyoxal neutralization during macrophage infection. Isogenic inactivation of *STM3117* in *S. Typhimurium* proved not to be lethal, alluding to the presence of either other detoxifying enzymes in the genome or sublethal concentrations of endogenous methylglyoxal under the conditions tested. Remarkably,  $\Delta$ *lgl* (deletion mutant of *STM3117*) was hypersensitive to growth inhibition by external methylglyoxal compared with WT (Fig. 1b). During growth in LB medium,  $\Delta$ *lgl* accumulated sublethal levels of endogenous methylglyoxal,  $12 \pm 0.3$  nmol (g wet weight)<sup>-1</sup>, compared with  $0.9 \pm 0.07$  nmol (g wet weight)<sup>-1</sup> of methylglyoxal produced by WT, as quantified by the levels of 2-methylquinoxaline (derivatized product of methylglyoxal) in HPLC. The reduced ability to degrade methylglyoxal resulted in the inhibition of growth of the mutant in the exponential growth phase. Enzymic activity also demonstrated that *STM3117* in the presence of the metal ion Co<sup>2+</sup> isomerized the methylglyoxal–GSH adduct hemithioacetal into S-D-lactoylglutathione (product) (Fig. 1c). The results validated the involvement of *STM3117* in methylglyoxal detoxification.

### Expression of *STM3117* results in differential replication of *S. Typhimurium* in phagocytic versus non-phagocytic cells

In order to investigate if *STM3117* was essential for intracellular survival, we compared the proliferation of  $\Delta$ *lgl* with WT in macrophages and epithelial cells. In murine macrophage line RAW264.7, an increased proliferation of ~30-fold was observed for the mutant compared with ~15-fold for WT (Fig. 2a). Similar trends were observed in human macrophage line U937 and murine BMDMs (Fig. 2a). Whilst complementation ( $\Delta$ *lgl*-pQE:*lgl*) restored the

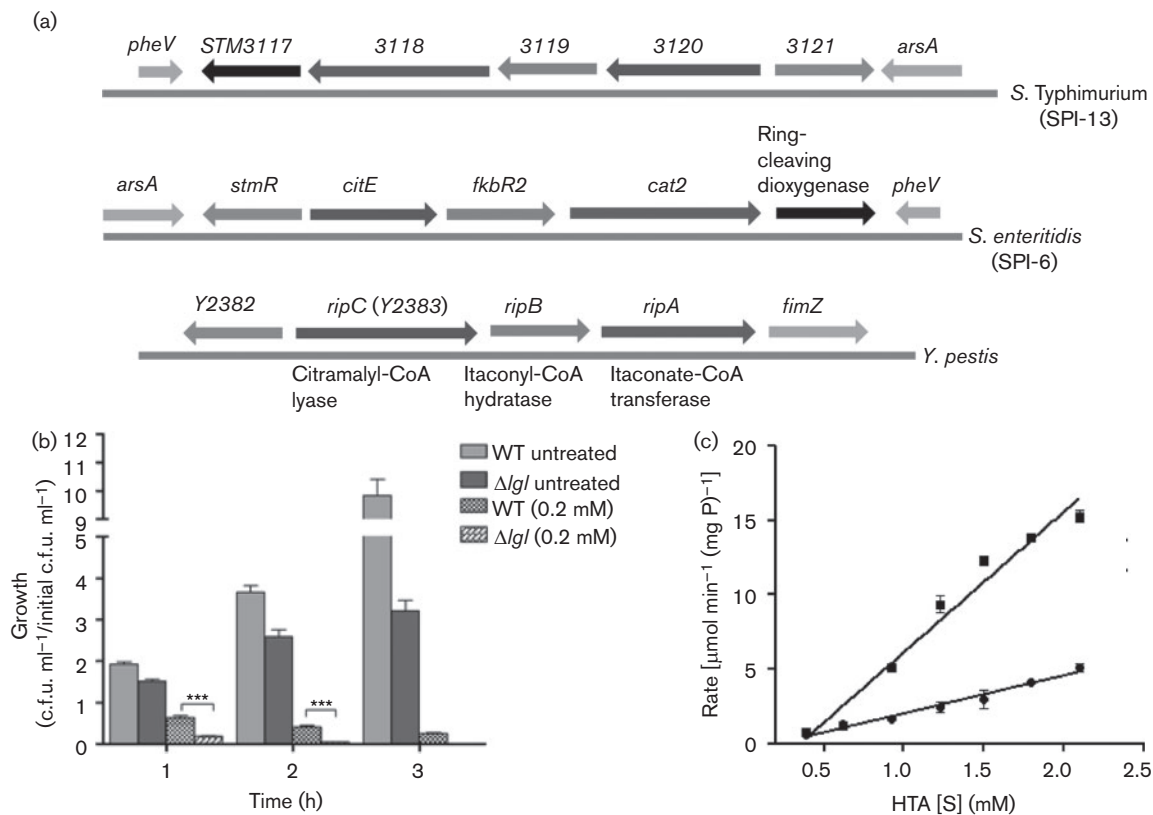


**Fig. 1.** (a) ORF map of the *STM3117–STM3121* locus in *S. Typhimurium*. Arrows depict the direction of transcription. The *rip* operon of *Yersinia pestis* and the corresponding homologous region of SPI-6 of *S. enteritidis* are compared. Similar coloured arrows represent the corresponding sequence homologues across species. In *Y. pestis* the *rip* operon genes have been recently annotated as per their substrate specific enzymatic activities. (b) Growth rate of bacteria with/without methylglyoxal (0.2 mM). Growth rate was calculated by dividing the c.f.u. ml<sup>-1</sup> by the initial c.f.u. ml<sup>-1</sup> every hour. Columns represent mean  $\pm$  SD of three independent experiments. \*\*\**P* < 0.001. (c) Activity of purified STM3117 enzyme of *S. Typhimurium* with (■) or without (●) divalent metal ions (Co<sup>2+</sup>). Initial rates were monitored by the increase in absorbance at 240 nm due to the conversion of hemithioacetal (HTA) to *S*-D-lactoylglutathione.

WT phenotype, the overexpressing strain  $\Delta lgl$ -pTrc:*lgl* exhibited an extremely low proliferation compared with the other strains. qRT-PCR analysis of *STM3117* expression confirmed that pTrc99c driven expression was ~15-fold higher than that from pQE60 (Fig. S1e, available in the online Supplementary Material). We hypothesized that the infection outcomes were affected by the critical level of STM3117 within bacteria, which when perturbed yielded differences in intracellular proliferation rates.  $\Delta lgl$  with empty pTrc99c control did not proliferate like  $\Delta lgl$  because LacI (Lac repressor) in pTrc99c reduces *Salmonella* virulence (Eswarappa *et al.*, 2009). Therefore, the proliferation defect of the overexpression strain observed in our gentamicin protection assays was the consequence of both LacI and excess STM3117-mediated repression of proliferation.

In cultured epithelial cell lines such as INT-407 and HeLa, the mutant exhibited a defective proliferation (Fig. 2b) along with reduced numbers of intracellular bacteria at 2 h

p.i (Fig. S1a). The invasion assay on epithelial cells revealed limited internalization of  $\Delta lgl$  in INT-407 (~9%) and CaCo-2 cells (~24%) compared with WT, whose internalization capacity was considered 100% (Fig. 2c). As the mutant showed restricted entry, we sought to determine the SPI-1 status in  $\Delta lgl$ . SPI-1-encoded TTSS-1 spans the bacterial membrane and helps translocate effector molecules across the host plasma membrane, where they cause active actin rearrangement and invasion (Lara-Tejero & Galán, 2009; Lostroh & Lee, 2001). qRT-PCR analyses and  $\beta$ -galactosidase reporter assay did not reveal any appreciable difference in the expression of the SPI-1 genes between the mutant and the WT (Fig. S1b, c). However, there was a significant decrease in the level of secreted SipC in the culture supernatant of the mutant (Fig. 2d), which was also reflected in the amount of translocated SipC from  $\Delta lgl$  into the host cell during invasion (Fig. S1d). The results showed a reduced ability of invasion of the mutant bacteria due to an impaired translocation of SPI-1 effectors.

Nonetheless, this indicated that the activity of STM3117 in intracellular *Salmonella* determines the extent of methylglyoxal detoxification, which additionally transpires to affect the proliferation rates within SCVs. The ability of the  $\Delta$ *lgl* mutant strain to replicate in the macrophages is in contrast to its replication defect in epithelial cells.

The capacity of  $\Delta$ *lgl* to colonize *in vivo* was also analysed. BALB/c and C57BL/6 mice were infected orally (Fig. 2e), and the former was also infected intraperitoneally (Fig. S1f). Compared with the WT-infected mice, which were moribund on day 4, the mutant-infected mice were active and showed minimal pathological symptoms of the disease. Both BALB/c and C57BL/6 mice showed ~75-fold minimized  $\Delta$ *lgl* burden in livers and spleens as compared with the WT. The mutant population manifested a systemic spread, albeit at a lower rate. Our results are in agreement with earlier reports on the inability of STM3117 (Santiviago *et al.*, 2009) or STM3117–3120 (Haneda *et al.*, 2009) mutants to survive *in vivo*. In fact, mice infected with such mutants show decreased morbidity and mortality (Haneda *et al.*, 2009; Shah *et al.*, 2005).

### Activity of *kefB* in response to the intracellular level of methylglyoxal–GSH adducts determines the proliferation rate of intramacrophagic *S. Typhimurium*

Proliferation dynamics of  $\Delta$ *lgl* within macrophages was in disagreement with the reported attenuation of this mutant inside macrophages (Shi *et al.*, 2006). We considered bacterial proliferation with respect to the SCV environment and SPI-2 activity, the two being key players in intracellular survival and growth, to resolve the ambiguity. First, we confirmed whether STM3117 detoxified methylglyoxal in intracellular *S. Typhimurium*.

In *E. coli*, the GSH conjugates of methylglyoxal, i.e. hemithioacetal and lactoylglutathione, induce potassium efflux channels (*kefB* and *kefC*) (Ferguson *et al.*, 1995). The channels work by effluxing  $K^+$  ions, with a simultaneous influx of  $H^+$  into the bacterial cytosol, whenever bacteria accumulate methylglyoxal–GSH adducts. Enhanced expression of *kefB* in the intramacrophagic mutant population indicated that *kefB* was elicited due to accumulated methylglyoxal–GSH adducts (Fig. 3a). The accumulation of toxic adducts in intracellular  $\Delta$ *lgl* was further confirmed by the increased induction of DNA *N*-glycosylases (*mutM*, *mutT* and *mutY* repair enzymes) (Fig. 3b). DNA repair enzymes had been previously speculated to become activated in response to low cytosolic pH (due to  $H^+$  influx) to rescue the bacteria from methylglyoxal-mediated DNA damage (Ferguson *et al.*, 1998). The question now was whether KefB antiported  $H^+$  from SCVs during the efflux of  $K^+$  ions. FACS analysis of the pH of MCVs revealed a significant increase in the mean fluorescence intensity of FITC (pH-sensitive probe) corresponding to pH 5.8 compared with WT-containing phagosomes (corresponding to pH 4.8) (Fig. 3c). FITC increases fluorescence upon an increase in

pH. Dual labelling of bacteria with a pH-sensitive dye (pHrodo with fluorescence maxima at acidic pH) and a pH-insensitive dye (Alexa Fluor 488) followed by infection yielded an increase in the mean pHrodo fluorescence intensity for WT SCVs as seen in the overlaid FACS histogram in Fig. 3(d). This again indicated that the pH of MCVs was less acidic than the WT SCVs. Mutant bacteria rapidly antiported phagosomal  $H^+$  by KefB to activate the repair enzymes.

The pH of epithelial cell SCVs, however, did not differ much between the WT and the mutant bacteria (Fig. S2), which indicated two possibilities – either KefB did not actively antiport  $H^+$  from MCVs or insufficient mutant bacteria resided within the endosomal vacuoles to give a net pH downshift. Moreover, epithelial cell SCVs are less acidic than macrophage SCVs (Hautefort *et al.*, 2008), which could also be a limiting factor for efficient KefB activity in the case of the mutant. To further validate that the increased proliferation of  $\Delta$ *lgl* in macrophages was mediated by KefB activity, we employed  $\Delta$ *kefB* and  $\Delta$ *lgl*/ $\Delta$ *kefB* mutant strains. The increased proliferation of  $\Delta$ *lgl* should be negated in a *kefB* mutant background. In accordance,  $\Delta$ *kefB* and the  $\Delta$ *lgl*/ $\Delta$ *kefB* double mutant had the same proliferative index in macrophages as in the WT (Fig. 3e). On the whole, the results showed that methylglyoxal detoxification was vital to survival within macrophages, which when impaired perturbs the dynamics of SCV pH.

### Rate of SPI-2 translocon secretion but not changes in expression level, accounts for the increased proliferation of $\Delta$ *lgl* in macrophages

Within host cells, a low pH (4–5) of the phagosomal compartment is considered to be an important cue for SPI-2 induction (Rathman *et al.*, 1996; Yu *et al.*, 2010). We have shown previously that MCVs of macrophages exhibited a higher pH than those of the WT SCVs due to the import of  $H^+$  from MCVs. We then hypothesized that a low pH of the bacterial cytosol ( $pH_{Bact}$ ) could enhance SPI-2 activity over and above the activity occurring due to phagosomal acidification.

When V-ATPase was inhibited with BAF to abolish vacuolar acidification in both RAW264.7 and INT-407 cells, a significant reduction in the net growth of  $\Delta$ *lgl* was observed in macrophages (Fig. 4a). It indicated that an acidic phagosomal niche is a prerequisite for the mutant to proliferate.

We quantified SPI-2 translocon proteins SseB and SseD, which are filament and pore-forming components of TTSS-2, respectively, and are secreted across the host phagosomal membrane in response to acidification (Hölzer & Hensel, 2010). Expression of *ssaP* and *ssaV* (SPI-2 genes) did not increase appreciably in intracellular  $\Delta$ *lgl*, indicating that the mutant's increased proliferation was not due to enhanced transcription of SPI-2 (Fig. 4b). Therefore, translocation of SPI-2 proteins was analysed to account for the enhanced

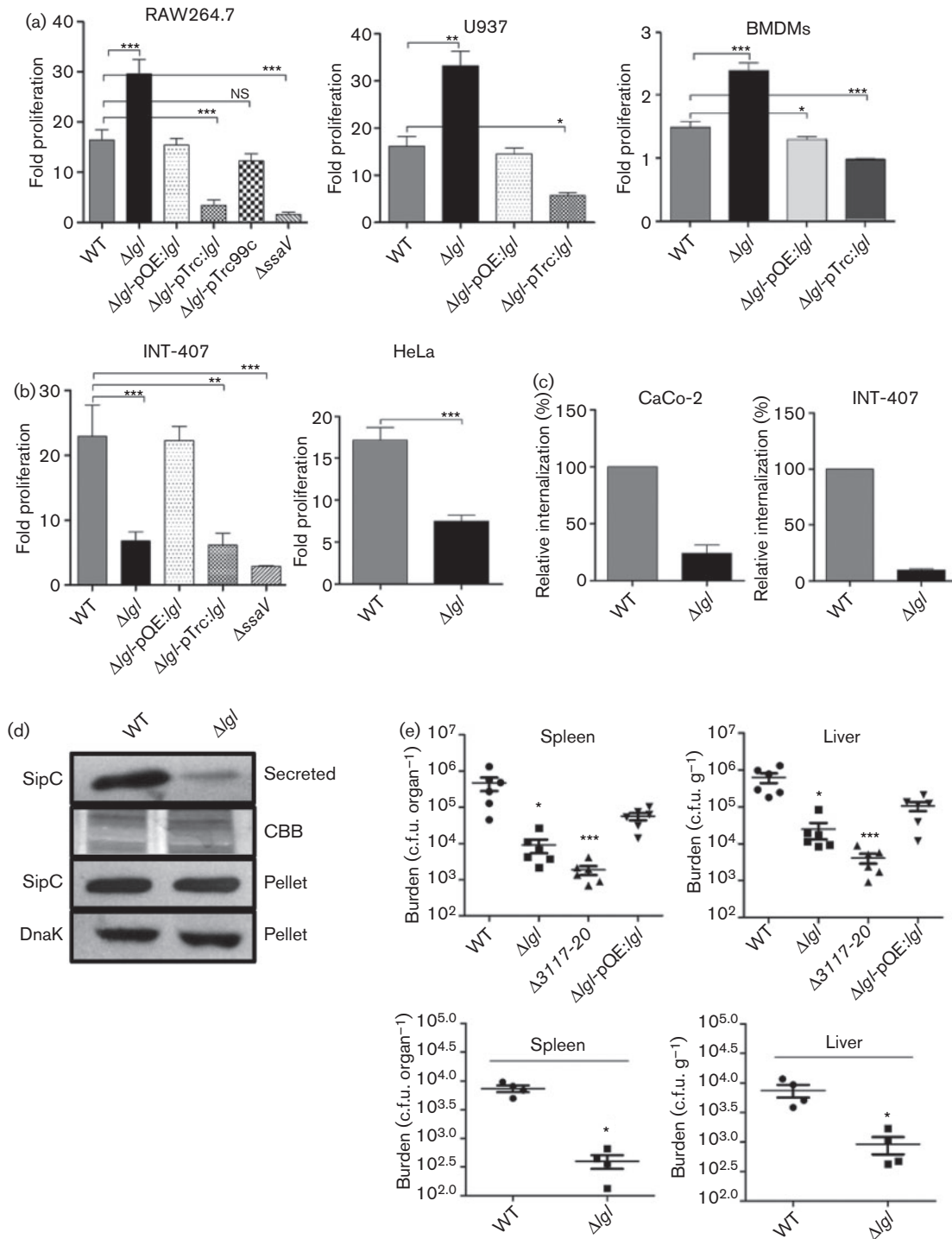


**Fig. 2.** Lactoylglutathione lyase contributes to intracellular proliferation and virulence. (a, b) Net intracellular replication of WT,  $\Delta lgl$ , complement strain ( $\Delta lgl$ -pQE:lgl) and overexpression strain ( $\Delta lgl$ -pTrc:lgl) from 2 to 16 h in RAW264.7 macrophages, U937 cells, murine BMDMs (a), and INT-407 and HeLa cells (b). In RAW264.7 cells the mutant with empty pTrc99c vector was kept as control to account for the virulence-lowering effect of the LacI repressor present in the vector.  $\Delta ssaV$  mutant was used as negative control. Each experiment was performed three times with each strain infecting the host cells in triplicate. The columns represent the mean  $\pm$  SEM from three different experiments. One-way ANOVA with Dunnett's *post hoc* analyses was used to compare the means relative to WT in intracellular proliferation assays. \* $P < 0.05$ ; \*\* $P < 0.01$ ; \*\*\* $P < 0.001$ ; NS, non-significant. (c) Per cent internalization of the indicated strains relative to the initial inocula in CaCo-2 and INT-407 cells. Values shown are the mean  $\pm$  SEM of three independent experiments. Student's *t*-test was used to compare the means. (d)

Representative immunoblot of SipC (SPI-1 effector) probed in culture supernatant (secreted) and whole-cell lysate (pellet). DnaK is used as a positive control for bacterial lysates. Coomassie brilliant blue (CBB) staining shows equal loading of samples. (e) Bacterial burden in spleens and livers of BALB/c (upper panel,  $n=6$ ) and C57Bl/6 (lower panel,  $n=4$ ) mice after 4 days of infection with an oral dose of  $10^6$  bacteria per mouse.  $\Delta 3117-20$  (deletion of the operon) strain with deletion of *STM3117-3120* genes was used as a negative control. The plots represent data from one experiment out of three independent experiments. The Kruskal–Wallis test was performed to calculate the statistical significance for BALB/c mice data and the Mann–Whitney *U* test was used for C57Bl/6 mice data.

replication of  $\Delta lgl$ . Bacteria grown in F-medium (SCV-like medium) (Eswarappa *et al.*, 2008) were processed for three different protein fractions: surface-attached, whole-cell lysate and whole-cell lysate without the surface-attached fraction.  $\Delta lgl$  showed an increased level of both SseB and SseD in the surface-attached protein fraction and whole-cell lysate (Figs 4c and S3), whereas the overexpression strain displayed a reduced amount, corresponding well with the earlier data on intracellular proliferation (Fig. 4c). However, in the whole-cell lysate fraction where the surface-attached proteins were removed prior to analysis, we found similar levels of the protein among the strains. This indicated that *STM3117* did not regulate the expression but negatively influenced transport across the TTSS-2 needle apparatus. Immunofluorescent detection of SseB and SseD in intramacrophage  $\Delta lgl$  and WT (Fig. 4d) further confirmed that there was no impairment whatsoever in expression of SPI-2 proteins in the mutant. The increased pH of  $\Delta lgl$ -containing phagosomes in macrophages in response to the metabolic status of the methylglyoxal–GSH conjugate presumably caused a lowering of the bacterial pH, which enhanced SPI-2 translocon secretion in  $\Delta lgl$ . However, within epithelial cells, the mutant failed to show detectable levels of SseD p.i. (Fig. 4d) as was expected due to poor proliferation. Based on these observations we believe that, beyond a threshold, *STM3117* concentrations negatively regulated translocation of SPI-2 proteins by some unknown mechanism, thereby disfavoured vacuolar replication of the overexpression strain. There is evidence of a positive regulatory effect of virulence factors on infection outcomes; nonetheless, there are cases where a pathogen needs to negatively regulate certain virulence factors to achieve steady-state dynamics within the host cells (Coombes *et al.*, 2005).

### STM3117 promotes maturation of SCVs

The proliferation defect of  $\Delta lgl$  in non-phagocytic cells cannot be due to poor SPI-2 activity alone since the impairment was observed at the downstream translocation stage and not at the expression stage (Fig. 4b, c). Also, in our studies with SPI-2 we observed a notable decrease in co-localisation of MCVs with the classical endocytic marker LAMP1 (Fig. 4d), which prompted us to believe that compromised vacuole maturation together with poor SPI-2 activity must be the cause of non-proliferative MCVs. As both EEA1 and LAMP1 are recruited sequentially onto the SCV membrane, and the latter is retained throughout the course of infection (Steele-Mortimer, 2008), we considered

bacterial co-localization with EEA1 and LAMP1 to be representative of SCV maturation.

In RAW264.7 macrophages, both  $\Delta lgl$  and WT showed similar co-localization with LAMP1 at 2 and 6 h (~70% co-localization) (Fig. 5a) and ~80% of the mutant bacteria co-localized with LAMP1<sup>+</sup> SCVs, similar to the WT (Fig. 5b). Co-localization of the non-LAMP1<sup>+</sup> bacteria with ubiquitinated aggregates early in infection (1 h p.i.) confirmed their cytosolic nature (Fig. S4a). The cytosolic population of *S. Typhimurium* is targeted by the ubiquitinated proteins which are further degraded by proteasome (Perrin *et al.*, 2004).

In INT-407 cells, however,  $\Delta lgl$  exhibited significantly decreased co-localization of 19, 30 and 42% with LAMP1 at 2, 6 and 12 h p.i., respectively (Fig. 5c). The amount of LAMP1 recruitment did not seem to increase even at late time points p.i. (12 h). Enumeration of the percentage of SCV-localized bacteria (LAMP1<sup>+</sup>) revealed 40–50%  $\Delta lgl$  in vacuoles with the rest in the cytosol (Fig. 5d). Co-localization of EEA1 was 20% with  $\Delta lgl$  compared with 80% with WT (Fig. 5e). Even at 1.5 h p.i., only a limited number of mutant bacteria had co-localized with EEA1.

To further determine if some of the mutant population escaped/quit MCVs to enter the cytosol and were cleared thereafter, we incorporated chloroquine ( $50 \mu\text{g ml}^{-1}$ ) in the gentamicin protection assay. The protonated form of chloroquine has the potential to kill vacuolar bacteria without any apparent effect on the cytosolic population (Marathe *et al.*, 2012). As shown in Fig. S4(b, c), the mutant population was predominantly vacuolar throughout infection in macrophages, whilst it was largely cytosolic at late time points within epithelial cells. This further indicated the poor maturation of MCVs within epithelial cells.

As epithelial cell cytosol is more permissive to bacterial replication than the macrophage, the former provides an ideal niche for *S. Typhimurium* to divide proficiently (Brumell *et al.*, 2002). However, the proliferation defect of the mutant within epithelial cells could not be due solely to immature MCVs, but due to targeting of these MCVs by the host defence system. Epithelial cells of various origin are known to express defensins such as HBD1, HBD3, HBD4 and HD5, which are potent AMPs and are known to kill pathogens by permeabilizing their cell membrane (Eswarappa *et al.*, 2008; Ganz, 2003). Immunofluorescence results showed a uniform distribution of HD5 in *S. Typhimurium*-infected INT-407 cells, and there was a visible increment in the co-localization of HD5 with the

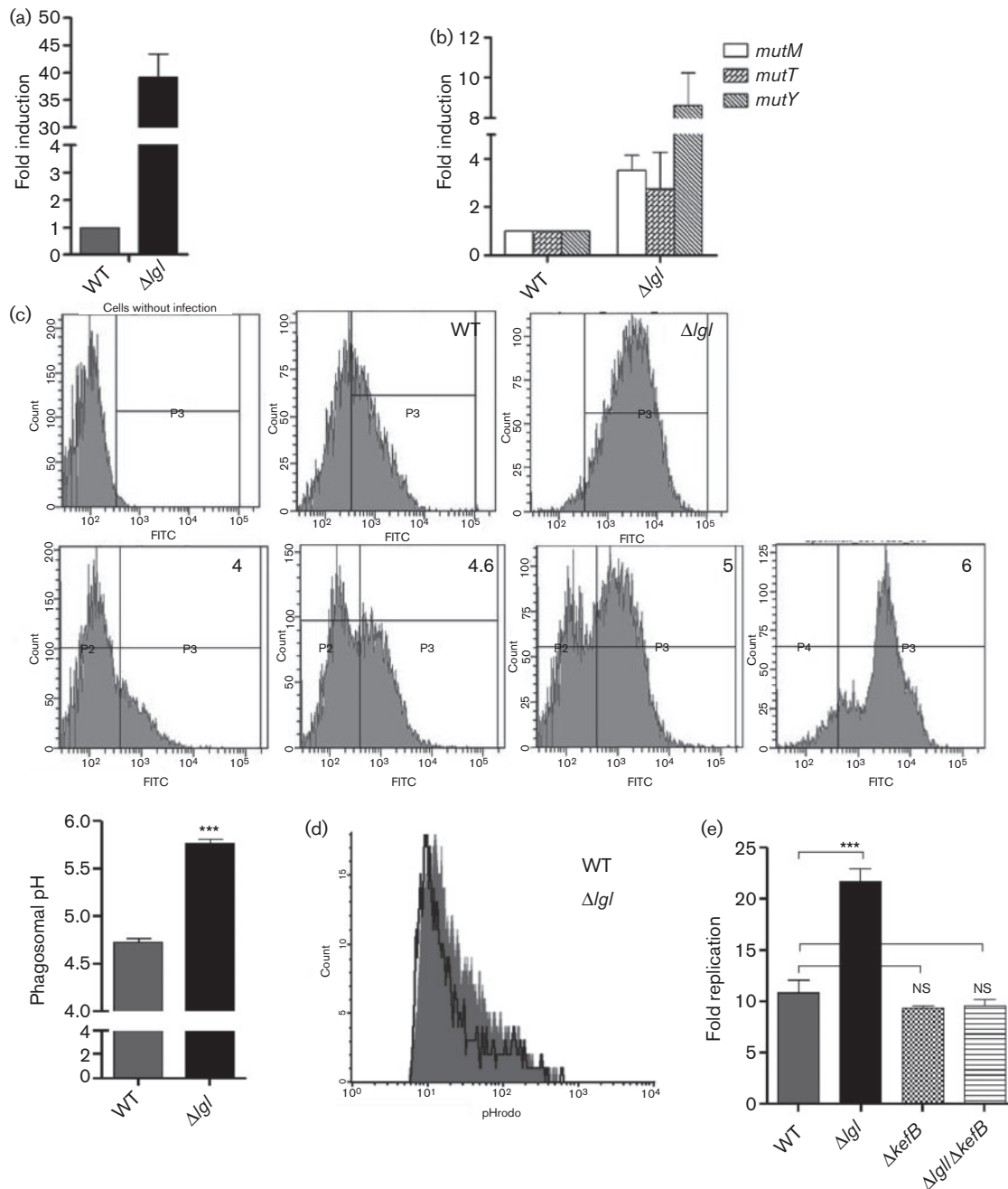


**Fig. 3.** Impaired intracellular methylglyoxal detoxification in macrophages increases the pH of  $\Delta Igl$ -containing SCVs more than that of WT SCVs. (a) qRT-PCR analysis of *kefB* in the indicated strains isolated from RAW264.7 macrophages at 4 h p.i. (b) Expression levels of *mutM*, *mutT* and *mutY* in intracellular  $\Delta Igl$  relative to that in WT (isolated from RAW264.7) cells at 5 h p.i. The plot is representative of three independent experiments performed in duplicates. Bar, SD. (c) Representative histograms of FITC fluorescence as per the phagosomal pH either with infection (FITC labelled WT and  $\Delta Igl$ ) alone or infection followed by equilibration with known pH buffers (4, 4.6, 5, 6) and nigericin. FITC (pH sensitive dye) labelled bacteria were allowed to infect RAW264.7 cells for 5 hr before harvesting samples for flow-cytometry. Equilibration was done for 30 min just prior to flowcytometric analysis. WT maintained a phagosomal pH  $\sim 4.8$ , whereas phagosomes of the  $\Delta Igl$  strain were less acidified and reached pH  $\sim 5.7$ . (d) Overlaid FACS histograms of pHrodo fluorescence intensity of the WT and  $\Delta Igl$ . pHrodo fluoresces at a maximum at acidified pH. Phagosomes containing WT show an increased fluorescence, indicating a relatively lower phagosomal pH than those of the  $\Delta Igl$ . Results of one independent experiment out of three is shown. (e) Net intracellular replication of WT,  $\Delta Igl$ ,  $\Delta kefB$  and  $\Delta Igl/\Delta kefB$  from 2 to 16 h in RAW264.7 macrophages. The columns represent the mean  $\pm$  SEM from three different experiments. One-way ANOVA with Dunnett's *post hoc* analyses was used to compare the means relative to WT in intracellular proliferation assays. \*\*\* $P < 0.001$ ; NS, non-significant.

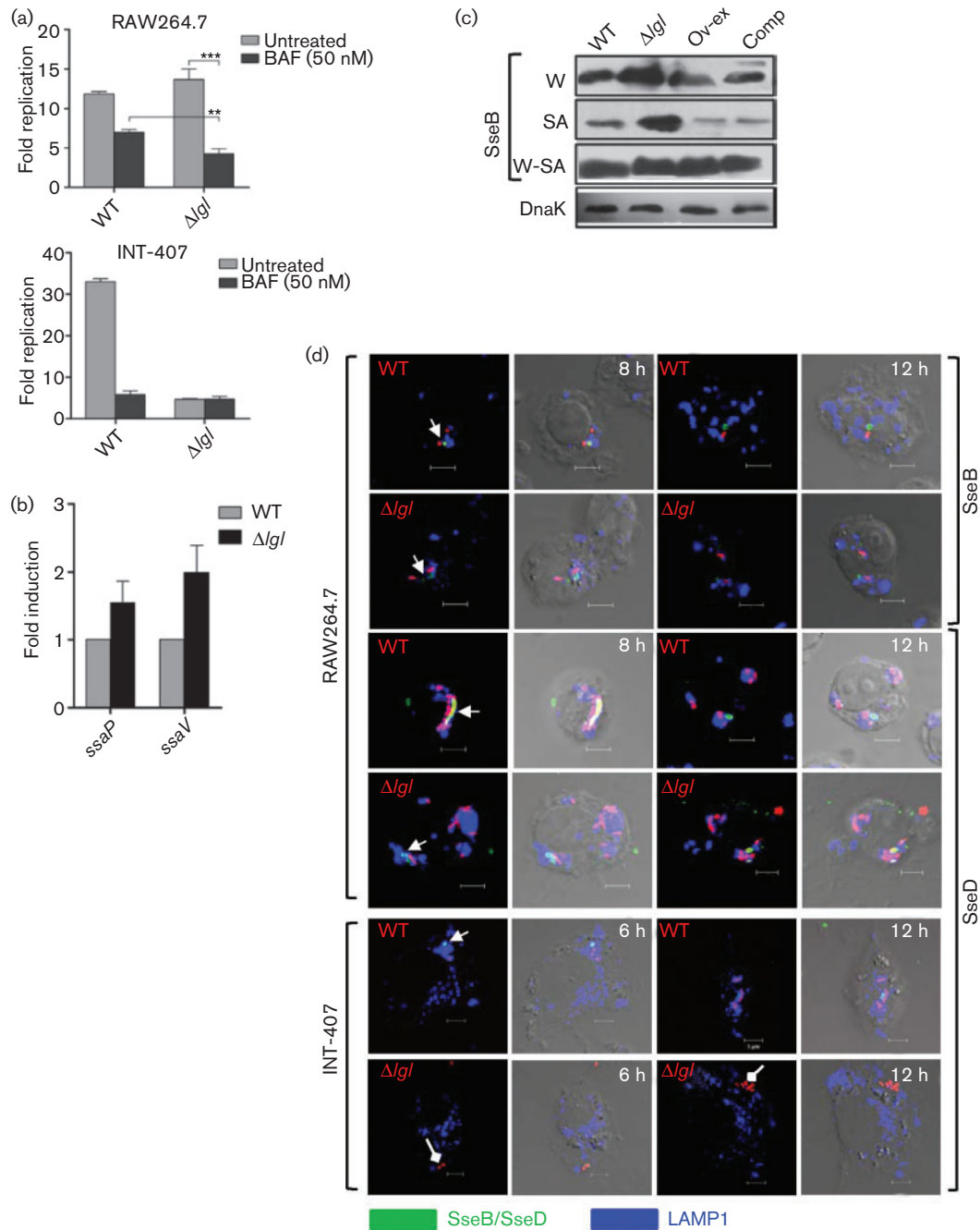
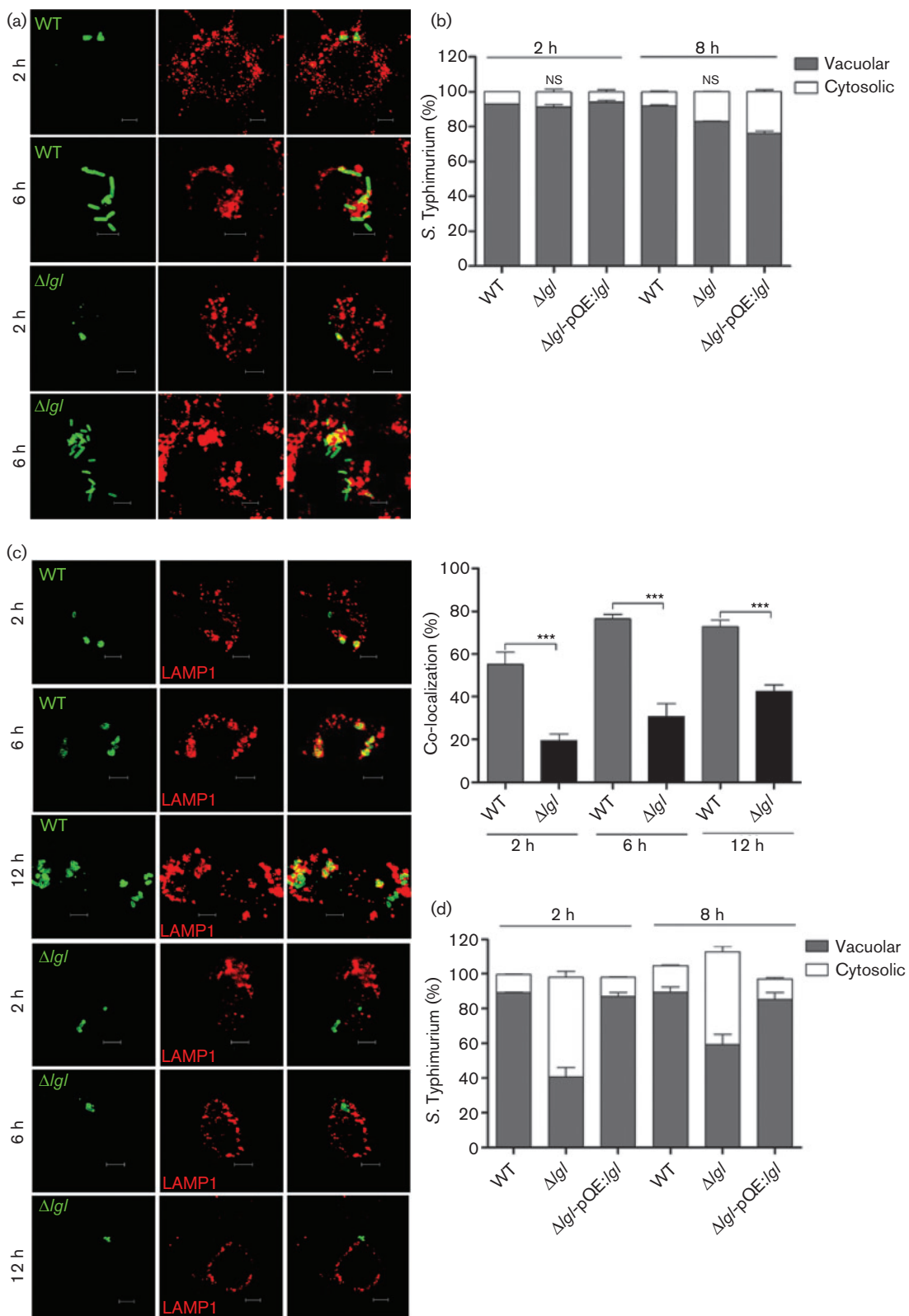


**Fig. 4.** SPI-2 translocon secretion increases in intramacrophage  $\Delta lgl$ . (a) RAW264.7 and INT-407 cells pretreated with BAF (50 nM) were infected with the indicated strain and the fold proliferation from 2 to 16 h was calculated. Graphs are representative of three independent experiments with similar results. Student's *t*-test was used to compare the means.  $**P < 0.01$ ;  $***P < 0.001$ . (b) qRT-PCR analysis of SPI-2 genes *ssaP* and *ssaV* in the indicated strains isolated from RAW264.7 macrophages at 4 h p.i. (c) Immunoblot analysis of SPI-2 translocon SseB from WT,  $\Delta lgl$ , complement strain (Comp;  $\Delta lgl$ -pQE:*lgl*) and overexpression strain (Ov-ex;  $\Delta lgl$ -pTrc:*lgl*) in whole-cell lysate (W), surface-attached fraction (SA) and cell lysate without the surface-attached fraction (W-SA). Strains were grown for 7 h in SPI-2-inducing medium (F-medium). (d) Single confocal sections of WT- and  $\Delta lgl$  (mCherry, red)-infected RAW264.7 and INT-407 cells, immunolabelled for SseB (green, arrowheads) and LAMP1 (blue, false coloured) at the indicated time points p.i.  $\Delta lgl$  inside INT-407 cells showed an absence of detectable levels of SseB and were frequently found not to co-localize with LAMP1 at both time points checked (diamond arrowheads). Bars, 5  $\mu$ m.



$\Delta Igl$  strain at 3 and 8 h p.i. (Fig. 5f). There was a significant increase in the sensitivity of the mutant to AMPs such as protamine and HBD1 during *in vitro* growth (Fig. S4d).

AMP-treated  $\Delta Igl$  was hypersensitive towards the treatment compared with the similarly treated WT, indicated by the increased incorporation of the membrane-potential-sensitive

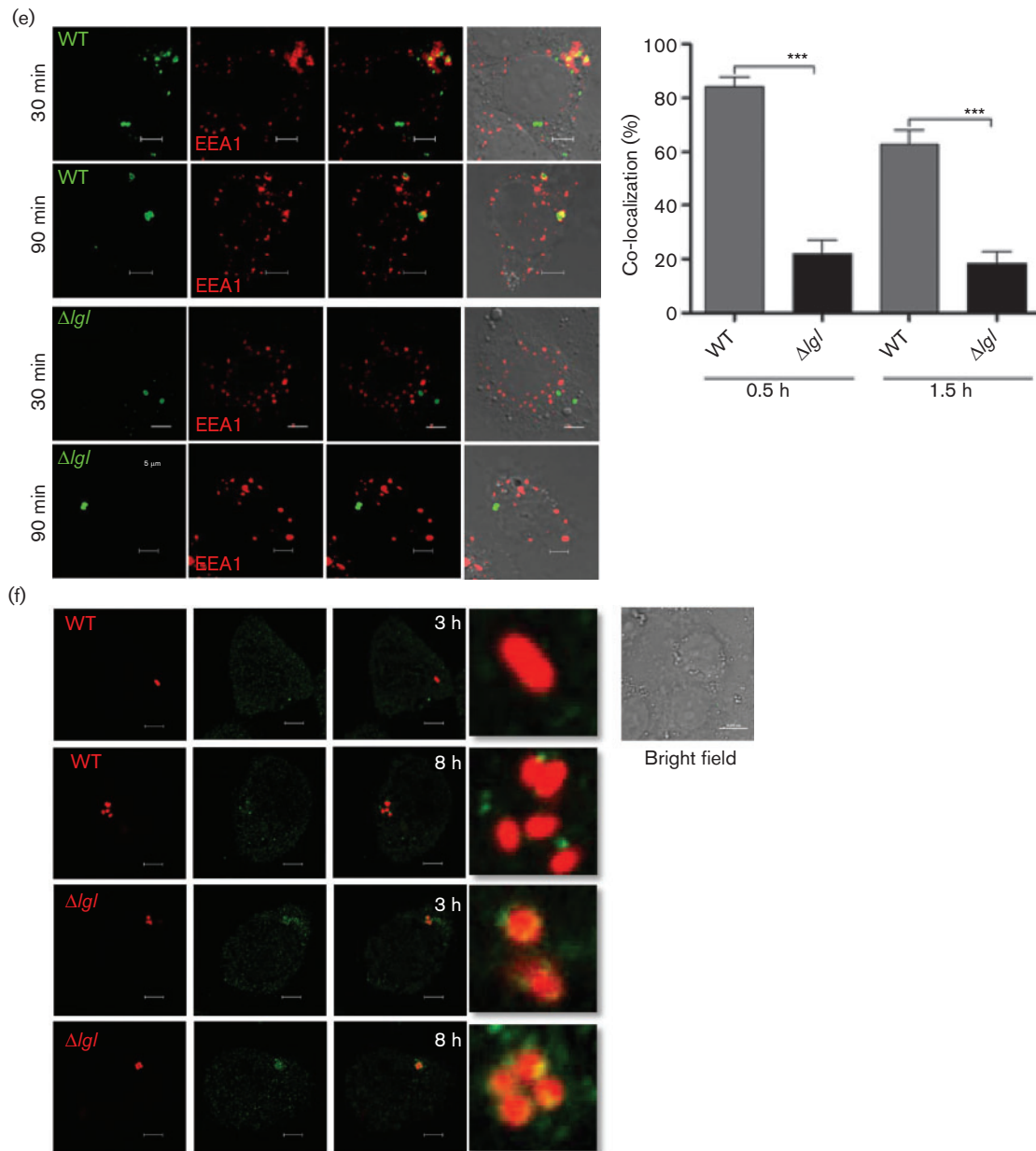


**Fig. 5.** The  $\Delta lgl$  population within epithelial cells exhibits defective SCV maturation and becomes susceptible to AMPs. (a–d) Single confocal sections of WT- and  $\Delta lgl$ -infected RAW264.7 (a) and INT-407 (c) cells at the indicated time points p.i. Bacteria were immunolabelled against *Salmonella* O-antigen and endosome marker LAMP1. Values represent the mean  $\pm$  SEM of per cent co-localization from three independent experiments each involving the analysis of 20 microscopic fields with 10–12 infected cells for each time point. Bar, 5  $\mu$ m. Percentage of bacteria (WT,  $\Delta lgl$  and complement) ( $n=200$ ) showing either  $>20$  (vacuolar) or  $\leq 20$  % (cytosolic) association with LAMP1 inside RAW264.7. \*\*\* $P<0.001$ . (b) and INT-407 (d) cells at 2 and 8 h p.i. Data are represented as mean  $\pm$  SEM of percentage of bacteria. NS, non-significant. (e) Single confocal sections of WT- and  $\Delta lgl$ -infected INT-407 cells at the indicated time points post-uptake, immunolabelled for EEA1 (red). Bars, 5  $\mu$ m (30 min); 5  $\mu$ m (90 min). Quantification of the per cent co-localization of bacteria with EEA1 is shown alongside the images, with values representing the mean  $\pm$  SEM of three independent experiments each involving the analysis of 50 infected cells for each time point. \*\*\* $P<0.001$ . (f) Co-localization of the indicated strains with HD5 in INT-407 cells at two time points p.i. Mutant bacteria exhibit increased susceptibility to HD5. Bars, 5  $\mu$ m.

dye DiBAC<sub>4</sub>(3) (Fig. S4e). The anionic dye is known to readily cross permeabilized/depolarized membranes and fluoresce. Thus, the amount of the membrane-potential-sensitive dye taken up by the AMP-treated cells would correlate directly with the loss of membrane integrity and depolarization (Nuding *et al.*, 2006). Altogether, the results show that within epithelial cells the mutant escapes from MCVs very early in infection and the fraction of  $\Delta lgl$  which manages to stay inside MCVs is subsequently targeted by AMPs, contributing to their decreased net growth.

### Expression of TLR2 and 4 partially restores the growth of the *STM3117* mutant inside epithelial cells

Recently, Denise Monack's group has revealed the importance of TLR signalling in recognition of intracellular *S. Typhimurium* (Arpaia *et al.*, 2011). They have shown that the presence of TLR2, 4 and 9 in mouse BMDMs is necessary for the establishment of an acidic phagosomal compartment and induction of SPI-2 genes in *Salmonella*. Moreover, epithelial SCVs are less acidic than macrophage SCVs. As primary intestinal epithelial cells are known to negligibly express TLR2 and 4 on their membranes, but constitutively express TLR3 and 5 (Cario & Podolsky, 2000; Hornef *et al.*, 2002), we used TLR-mediated signalling in epithelial cells to mimic the phagosomal environment of macrophages. We showed a lower expression of TLR4 in INT-407 cells compared with that in macrophages (Fig. 6a), and hence used FLAG-tagged human TLRs (TLR2 4) for transient transfections of INT-407 cells (Fig. S5a). Expression of either TLR did not suffice in restoring vacuolar localization of the mutant (Fig. S5b). However, INT-407 cells expressing both human TLR2 and 4 exhibited a significant increase in SCV localization of the mutant by 8 h p.i (Fig. 6b, c). Also, the proliferation of  $\Delta lgl$  increased significantly in transfected cells relative to that in the vector control (Fig. 6d). Transfected epithelial cells pretreated with BAF showed an intermediate proliferation rate in between that of inhibitor alone and transfection alone, further validating the role of TLR signalling in enhancing endosomal acidification in otherwise lower acidic endosomes of epithelial cells and proliferation thereof.

Conversely, RAW264.7 cells transfected with the dominant-negative mutant forms of mouse TLR2 and 4 resulted in ~40% of both WT and  $\Delta lgl$  in the cytosol (Fig. 6e, f). Dominant-negative forms of mouse TLRs impaired the optimal phagosomal acidification which would have served as a H<sup>+</sup> source for the mutant during methylglyoxal detoxification. These results demonstrated the interplay between SPI-2 translocon secretion in intracellular *S. Typhimurium*, induced by H<sup>+</sup> quenching from the surrounding acidified phagosomes.

## DISCUSSION

Methylglyoxal, a toxic byproduct of many physiological reactions (Chauhan & Madhubala, 2009; Kim *et al.*, 2012;

Korithoski *et al.*, 2007; MacLean *et al.*, 1998; Yadav *et al.*, 2005), arises primarily through various metabolic pathways, e.g. increased glycolytic flux of triose phosphates, threonine/glycine catabolism and acetone breakdown (Ferguson *et al.*, 1998). However, regardless of the pathway of methylglyoxal formation, the detoxification is exclusively dependent on cellular glyoxalases (Ferguson *et al.*, 1995; Korithoski *et al.*, 2007; Ozyamak *et al.*, 2010). The presence of a lactoylglutathione lyase (a putative glyoxalase I) gene in *S. enterica* serovar Typhimurium, Enteritidis, Gallinarum and other non-typhoidal serovars, but absence in typhoidal serovars might be indicative of host-specific acquisition of virulence determinants and metabolic requirements (Charles *et al.*, 2009; Pujol *et al.*, 2005; Rathman *et al.*, 1996). The non-phylogenetic distribution of the homologues of coding regions downstream of *STM3117*, i.e. *STM3118–3121*, in other species such as *Pseudomonas aeruginosa*, *Coxiella burnetii*, *Mycoplasma synoviae* and *Yersinia pestis*, indicate their acquisition through horizontal transfer. For instance, in *Y. pestis*, the *rip* operon genes (*ripA*, putative CoA transferase; *ripB*, putative monoamine oxidase; Y2383, putative citrate lyase  $\beta$  chain; Y2382, transcriptional regulator), which are homologues of the *STM3118–3121* cluster, are involved in reducing nitric oxide levels within macrophages in order to persist in activated macrophages (Pujol *et al.*, 2005). Recently, the *rip* operon genes, (Y2383–2385; Y2383 being annotated as *ripC* recently) have been shown to be involved in a step-by-step degradation of itaconate – an antimicrobial macrophage factor (Sasikaran *et al.*, 2014). However, the corresponding homologue sequence of *STM3117* does not exist in these pathogens.

Why an additional methylglyoxal degradation gene is present in non-typhoidal *Salmonella* serovars is something which is difficult to analyse at present based on the available literature and our own findings. However, we do see a decrease in intracellular proliferation of *S. Typhi* expressing *STM3117* compared with WT *S. Typhi* in human macrophages and epithelial cells (data not shown), revealing that *STM3117* apparently does not provide any proliferative advantage to *S. Typhi*. In *S. Typhimurium*, however, *STM3117* had a profound effect on the intracellular proliferation that was mediated by the activity of KefB and SPI-2. SPI-2-encoded TTSS-2 predominantly modulates intracellular proliferation in *S. Typhimurium* (Brown *et al.*, 2005; Dandekar *et al.*, 2012; Hölzer & Hensel, 2010; Jantsch *et al.*, 2011). The apparatus translocates proteins that mediate SCV maturation by positioning the SCV at the juxtannuclear site, making it a proliferation-productive niche (Steele-Mortimer, 2008). Whilst secretion of SPI-2 translocon components such as SseB and SseD was greatly enhanced in  $\Delta lgl$ , there was no difference in the expression of SPI-2 needle apparatus genes such as *ssaV* and *ssaP* (Fig. 3b) between WT and the mutant. SPI-2 activity was demonstrated to be modulated by the intracellular level of *STM3117* by using low ( $\Delta lgl$ -pQE60: *lgl*) and high ( $\Delta lgl$ -pTrc: *lgl*) expression strains of *STM3117* (Fig. 3).

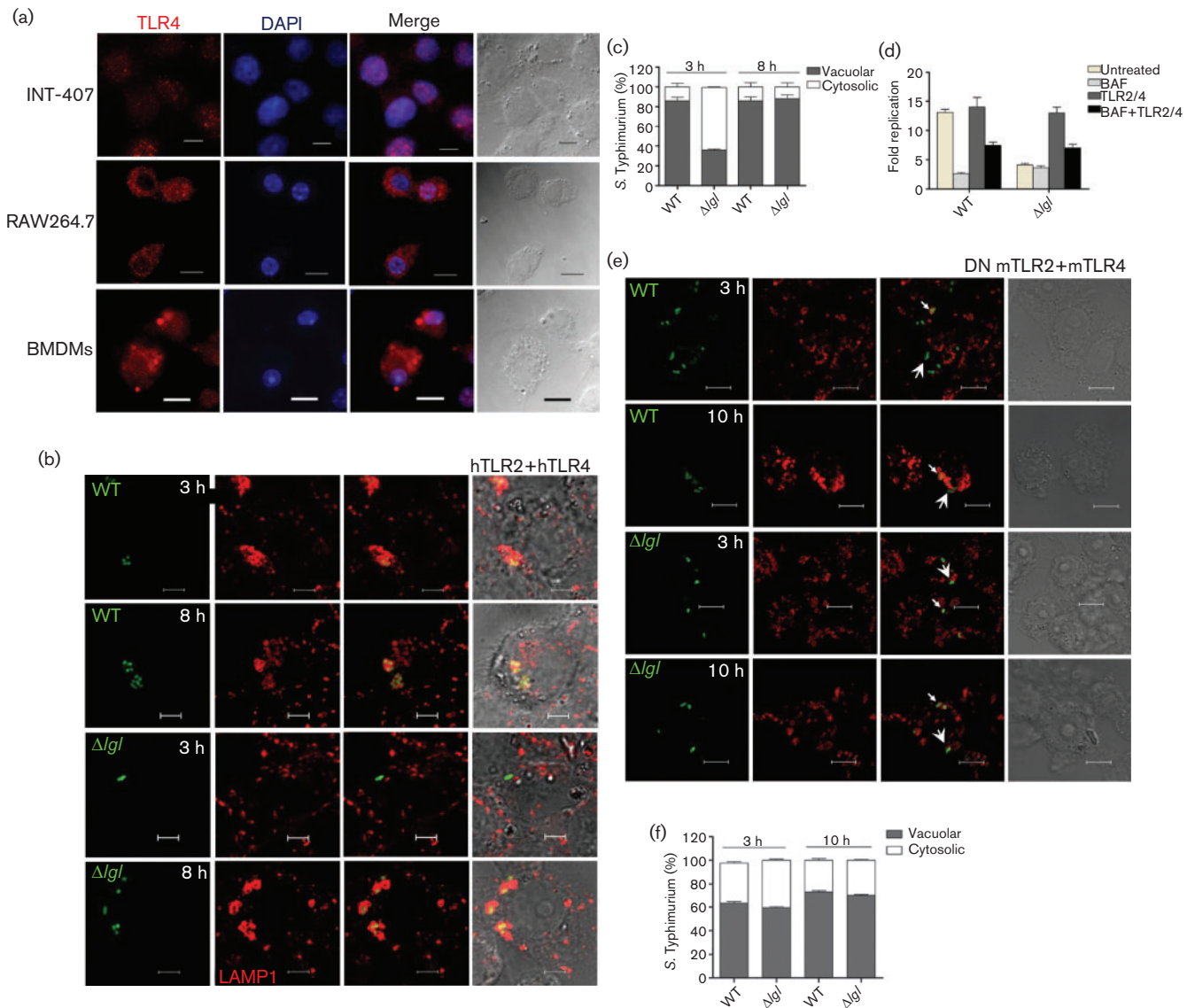


**Fig. 6.** TLR signalling rescues the proliferation defect of  $\Delta lgl$  in epithelial cells. (a) Fluorescent images of the indicated cells showing TLR4 expression (human TLR4 for INT-407 cells, and mouse TLR4 for RAW264.7 and BMDMs). Bars, 5  $\mu\text{m}$ . (b) Single confocal sections of WT- and  $\Delta lgl$ -infected INT-407 cells transfected with human (h) TLR2 and 4 at the indicated time points. The images are representative of three independent experiments. Bars, 5  $\mu\text{m}$ . (c) Percentage of WT and  $\Delta lgl$  ( $n=200$ ) showing either >20% (vacuolar) or  $\leq 20\%$  (cytosolic) association with LAMP1 inside transfected (with human TLR2 and 4) INT-407 cells at 2 and 8 h. Data are represented as mean  $\pm$  SEM of percentage of bacteria. (d) Net intracellular replication of WT and  $\Delta lgl$  in INT-407 cells under different conditions. Transfected or vector-transfected cells were either pretreated for 1 h with BAF (50 nM) or mock treated. Results are shown as mean  $\pm$  SEM of three independent experiments. (e) Single confocal sections of WT- and  $\Delta lgl$ -infected RAW264.7 cells transfected with dominant-negative (DN) forms of mouse (m) TLR2 and 4 at the indicated time points post-phagocytosis. The images are representative of three independent experiments. Small arrowheads indicate vacuolar bacteria and big arrowheads indicate the cytosolic population. Bars, 10  $\mu\text{m}$ . (f) The percentage of WT and  $\Delta lgl$  ( $n=200$ ) showing >20% (vacuolar) or  $\leq 20\%$  (cytosolic) association with LAMP1 inside dominant-negative mouse TLR2- and 4-transfected RAW264.7 cells at 3 and 10 h. Data are represented as mean  $\pm$  SEM of percentage of bacteria.

The exact cues for SPI-2 translocon secretion are still debated, and there exists a complex coordination between bacterial virulence factors and the host microenvironment

which together decide the fate of SPI-2 function and proliferation (Brown *et al.*, 2005; Coombes *et al.*, 2005; Dieye *et al.*, 2009). Bacteria grown in acidic media show

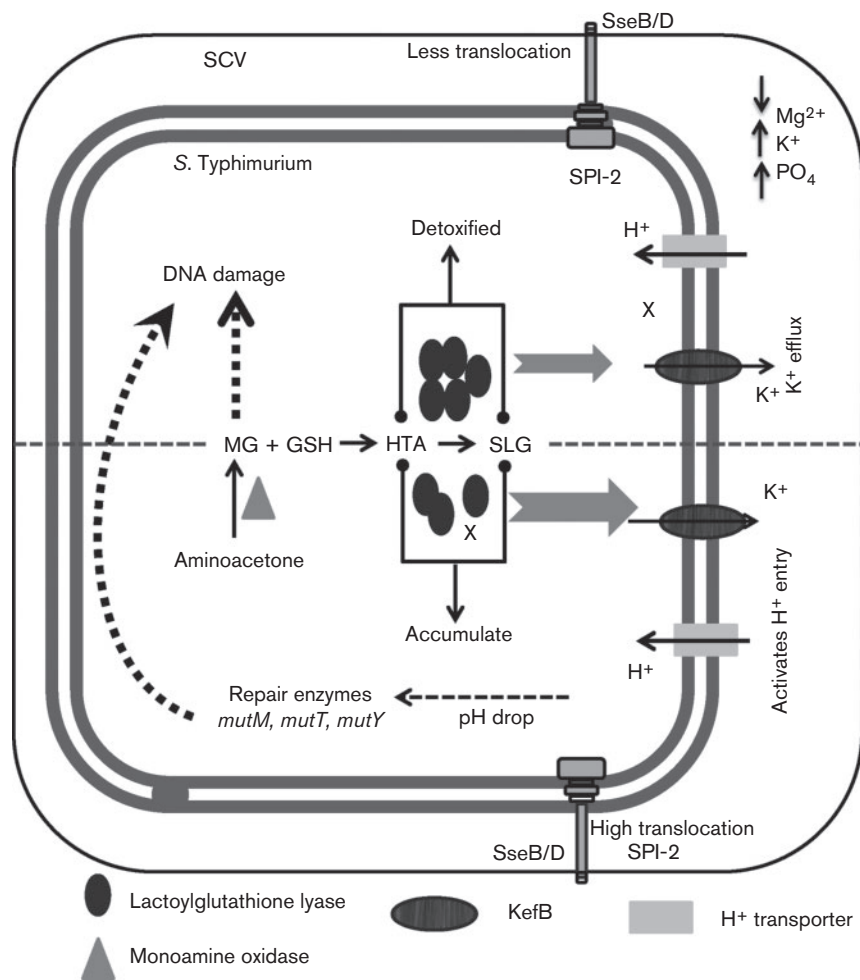


**Fig. 7.** A schematic representation of the possible outcomes of intracellular proliferation within the macrophage. Two possible outcomes are shown: one where abundant STM3117 is present (in the overexpression strain, top portion above the dashed mid line) and methylglyoxal (MG) is readily detoxified, and the other where STM3117 is absent or present in low copy (in  $\Delta gl$  or complement, below the dashed mid line) and methylglyoxal-GSH conjugates accumulate. The thickness of the fork-tailed grey arrows shows the strength with which the KefB channel is elicited, which is more when the toxic adducts accumulate. Thick dotted arrows show the participation of repair enzymes in preventing DNA damage caused as a result of methylglyoxal adduct accumulation. HTA, hemithioacetal; SLG, S-D-lactoylglutathione.

effective secretion of SPI-2 effectors and translocon components in a SsrB-dependent manner (Coombes *et al.*, 2004). We predicted that an acidified bacterial cytosol could boost the SPI-2 translocon secretion further than the extent achieved by sensing of acidic phagosomes (Fig. 7). The hypothesis was based on the fact that cytoplasmic acidification in *E. coli* (Ferguson & Booth, 1998; Ferguson *et al.*, 1995) happens in response to metabolite detoxification. The  $H^+$ -mediated pH drop essentially gives bacteria a short time to adapt and activate the repair system in response to methylglyoxal toxicity (Ferguson *et al.*, 1998), which was validated in our case by the induction of DNA repair enzymes (*N*-glycosylases), such as *mutM*, *mutY* and *mutT*, and the  $K^+$  efflux pump *kefB* in intracellular  $\Delta gl$  (Figs 3a, b and 7). Therefore, the enhanced secretion of

SPI-2 translocon components in the mutant could be explained by considering KefB mediated lowering of  $pH_{Bact}$  (Fig. 4). This fact was further substantiated by the presence of mildly acidic MCVs in macrophages ( $\sim pH_{5.7}$ ) (Fig. 3c). The mutant bacteria of MCVs actively import  $H^+$  ions (through KefB activity) from the phagosomes in response to the toxicity of the methylglyoxal-GSH adducts. The role of *kefB* in mediating this event was also confirmed by using  $\Delta kefB$  and  $\Delta gl/\Delta kefB$  double-knockout strains, both of which behaved similar to the WT (Fig. 2e)

TTSS-2 is located in the bacterial membrane in such a way that the regulatory complex of SsaL/SsaM/SpiC interacts with the basal body of the needle apparatus and responds to subtle changes in the host cytosolic pH ( $pH_{Cyt}$ ) through the action of an unknown pH sensor (Yu *et al.*, 2010). A

low  $\text{pH}_{\text{Cyt}}$  (pH-5) has been suggested to strongly induce translocon secretion but suppress effector delivery while a near neutral pH is shown to trigger effector delivery. Yu *et al.* (2010) reported that a certain bacterial pH sensor could be sensing these changes and regulating the activity of SsaL/SsaM/SpiC complex, where in, dissociation of the complex happens at a near neutral  $\text{pH}_{\text{Cyt}}$  followed by effector delivery. What has not been discussed is whether this unknown bacterial pH sensor also senses host phagosomal pH ( $\text{pH}_{\text{Phag}}$ ) and bacterial cytosolic pH ( $\text{pH}_{\text{Bact}}$ ). This question arises based on the fact that the TTSS-2 regulatory complex at the cytoplasmic side of the needle apparatus is directly under the influence of bacterial cytosolic pH. It is plausible therefore, that the intramacrophagic mutant bacteria with more acidic  $\text{pH}_{\text{Bact}}$  first strongly induces translocon secretion and as the  $\text{pH}_{\text{Phag}}$  increases (at 5 hr p.i. pH 5.7 vs pH 4.8 for WT) the regulatory complex triggers robust effector secretion by dissociating from the TTSS-2. Thus the interplay of  $\text{pH}_{\text{Bact}}$ ,  $\text{pH}_{\text{Phag}}$  and  $\text{pH}_{\text{Cyt}}$  together determines the fate of SPI-2 activity.

Epithelial SCVs require additional TLR-mediated signalling to achieve macrophage SCV-like characteristics. It is known that macrophage SCVs are more acidic in nature than epithelial SCVs (Hautefort *et al.*, 2008). For instance, TLR2-, 4- and 9-mediated acidification of phagosomes is required for SPI-2 induction in *S. Typhimurium* (Arpaia *et al.*, 2011). Interestingly, epithelial cells transfected with both human TLR2 and 4 partially rescued the intracellular proliferation of the mutant (Fig. 5b, d) by preventing their escape from the acidified SCVs. Insufficiently acidified SCVs of naive epithelial cells limited the extent of SPI-2 translocon secretion in  $\Delta\text{Igl}$ , which translated to a defective proliferation. However, post-transfection with TLRs, the proportion of vacuolar  $\Delta\text{Igl}$  and their proliferation increased. Conversely, RAW264.7 cells expressing dominant-inhibitory forms of mouse TLR2 and 4 resulted in ~30% of both WT and  $\Delta\text{Igl}$  outside phagosomes, reinforcing the importance of phagosomal acidification in the initial stages of infection (Fig. 5e, f). These findings further strengthen the fact that  $\text{pH}_{\text{Cyt}}$ ,  $\text{pH}_{\text{Phag}}$  and  $\text{pH}_{\text{Bact}}$  together influence the intracellular *Salmonella* proliferation and infection outcome.

Acid resistance genes become upregulated up to 10-fold in *S. flexneri* in response to low cytosolic pH of U937 cells compared with only twofold in HeLa cells (Lucchini *et al.*, 2005). Such observations further reiterate the influence of the immediate environment (vacuole or cytosol) of a particular pathogen on the expression of virulence genes. Similarly, in *S. Typhimurium*, the genes from *STM3117* to *STM3120* are also highly expressed in macrophages (Eriksson *et al.*, 2003), but are downregulated in HeLa cells (Hautefort *et al.*, 2008); which certainly does not exclude their requirement in intraepithelial proliferation. Contrary to an existing report suggesting *STM3117*'s role in peptidoglycan synthesis, we found that the enzyme has glyoxalase I activity and is involved in methylglyoxal detoxification. Moreover, the *STM3117* mutant did not reveal any defect

in cell wall integrity or sensitivity to certain detergents (data not shown), further supporting the notion that the encoded enzyme is not involved in peptidoglycan synthesis pathway.

One interesting observation from this study was the apparent difference in the mutant's behaviour *in vitro* and *in vivo* (Fig. 1a, e). Although our observations on mouse infection were in full agreement with previous work showing the inability of either *STM3117* or *STM3117-3120* mutants to cause infection or survive *in vivo*, the results on macrophage infection differed widely. As the *STM3117* mutant maintained a non-proliferative phenotype in epithelial cells as well as had low internalization efficiency (Fig. 1b, c), this could account for one of the reasons behind failure of the mutant to gain entry through the intestinal epithelia. However, due to the mutant's ability to replicate successfully within macrophages, we observed a systemic dissemination of the mutant in the livers and spleens of mice because  $\text{CD18}^+$  phagocytes are the major carriers of *Salmonella in vivo* (Cano *et al.*, 2001). The net outcome of the infection, however, was not detrimental to the host as the initial number of mutants translocating the gut epithelia itself was low. Further investigation is required to understand the intramacrophage mutant population *in vivo* and its contribution to the observed systemic spread.

Our results unravelled an important role of lactoylglutathione lyase in *S. Typhimurium* infection, and established the impact of metabolite detoxification on vacuole maturation dynamics. Our findings showed how the events of metabolite detoxification influence the acidification status of SCVs and vice versa, which ultimately translates to the infection outcome. Determining the subtleties of acidification and pH regulation in phagosomes and cytosol will promote studies on other intracellular pathogens which are known to modulate their virulence factors to combat the pH-based differences in their micro-environment.

## ACKNOWLEDGEMENTS

We thank Professor Michael Hensel (University of Osnabruck, Germany) for the *S. Typhimurium* strain. We would like to thank Samrajyam for helping us with the immunofluorescence analysis, and Sandeepa, Amit and Arvindhan for careful reading of the manuscript. We thank the Electron Microscopy Facility and Flow Cytometry Facility for help. We would like to thank the Central Animal Facility for providing the animals. This work was supported by the Director of the Indian Institute of Science, Bangalore, India [grant Provision (2A) Tenth Plan (191/MCB)], Department of Biotechnology (DBT 311, NBA, sanctioned by the President), Life Science Research Board (LSRB0008) and DBT-IISc Partnership Program for Advanced Research in Biological Sciences and Bioengineering to D.C. Infrastructure support from the Indian Council of Medical Research (Center for Advanced Study in Molecular Medicine), Department of Science and Technology (Fund for Improvement of S&T Infrastructure), and University Grants Commission (special assistance) is acknowledged. S.C., D.C. and A.B. acknowledge the Council of Scientific and Industrial Research for fellowships.

## REFERENCES

- Arpaia, N., Godec, J., Lau, L., Sivick, K. E., McLaughlin, L. M., Jones, M. B., Dracheva, T., Peterson, S. N., Monack, D. M. & Barton, G. M. (2011). TLR signaling is required for *Salmonella typhimurium* virulence. *Cell* **144**, 675–688.
- Bernardo, J., Long, H. J. & Simons, E. R. (2010). Initial cytoplasmic and phagosomal consequences of human neutrophil exposure to *Staphylococcus epidermidis*. *Cytometry A* **77**, 243–252.
- Booth, I. R., Ferguson, G. P., Miller, S., Li, C., Gunasekera, B. & Kinghorn, S. (2003). Bacterial production of methylglyoxal: a survival strategy or death by misadventure? *Biochem Soc Trans* **31**, 1406–1408.
- Brown, N. F., Vallance, B. A., Coombes, B. K., Valdez, Y., Coburn, B. A. & Finlay, B. B. (2005). *Salmonella* pathogenicity island 2 is expressed prior to penetrating the intestine. *PLoS Pathog* **1**, e32.
- Brumell, J. H., Tang, P., Zaharik, M. L. & Finlay, B. B. (2002). Disruption of the *Salmonella*-containing vacuole leads to increased replication of *Salmonella enterica* serovar Typhimurium in the cytosol of epithelial cells. *Infect Immun* **70**, 3264–3270.
- Campos-Bermudez, V. A., Leite, N. R., Krog, R., Costa-Filho, A. J., Soncini, F. C., Oliva, G. & Vila, A. J. (2007). Biochemical and structural characterization of *Salmonella typhimurium* glyoxalase II: new insights into metal ion selectivity. *Biochemistry* **46**, 11069–11079.
- Cano, D. A., Martínez-Moya, M., Pucciarelli, M. G., Groisman, E. A., Casadesús, J. & García-Del Portillo, F. (2001). *Salmonella enterica* serovar Typhimurium response involved in attenuation of pathogen intracellular proliferation. *Infect Immun* **69**, 6463–6474.
- Cario, E. & Podolsky, D. K. (2000). Differential alteration in intestinal epithelial cell expression of Toll-like receptor 3 (TLR3) and TLR4 in inflammatory bowel disease. *Infect Immun* **68**, 7010–7017.
- Chakravorty, D., Hansen-Wester, I. & Hensel, M. (2002). *Salmonella* pathogenicity island 2 mediates protection of intracellular *Salmonella* from reactive nitrogen intermediates. *J Exp Med* **195**, 1155–1166.
- Charles, R. C., Harris, J. B., Chase, M. R., Lebrun, L. M., Sheikh, A., LaRocque, R. C., Logvinenko, T., Rollins, S. M., Tarique, A. & other authors (2009). Comparative proteomic analysis of the PhoP regulon in *Salmonella enterica* serovar Typhi versus Typhimurium. *PLoS ONE* **4**, e6994.
- Chauhan, S. C. & Madhubala, R. (2009). Glyoxalase I gene deletion mutants of *Leishmania donovani* exhibit reduced methylglyoxal detoxification. *PLoS ONE* **4**, e6805.
- Clugston, S. L., Yajima, R. & Honek, J. F. (2004). Investigation of metal binding and activation of *Escherichia coli* glyoxalase I: kinetic, thermodynamic and mutagenesis studies. *Biochem J* **377**, 309–316.
- Coombes, B. K., Brown, N. F., Valdez, Y., Brumell, J. H. & Finlay, B. B. (2004). Expression and secretion of *Salmonella* pathogenicity island-2 virulence genes in response to acidification exhibit differential requirements of a functional type III secretion apparatus and SsaL. *J Biol Chem* **279**, 49804–49815.
- Coombes, B. K., Wickham, M. E., Lowden, M. J., Brown, N. F. & Finlay, B. B. (2005). Negative regulation of *Salmonella* pathogenicity island 2 is required for contextual control of virulence during typhoid. *Proc Natl Acad Sci U S A* **102**, 17460–17465.
- Cordeiro, C. & Ponces Freire, A. (1996). Methylglyoxal assay in cells as 2-methylquinoxaline using 1,2-diaminobenzene as derivatizing reagent. *Anal Biochem* **234**, 221–224.
- Dandekar, T., Astrid, F., Jasmin, P. & Hensel, M. (2012). *Salmonella enterica*: a surprisingly well-adapted intracellular lifestyle. *Front Microbiol* **3**, 164.
- Das, P., Lahiri, A., Lahiri, A., Sen, M., Iyer, N., Kapoor, N., Balaji, K. N. & Chakravorty, D. (2010). Cationic amino acid transporters and *Salmonella* Typhimurium ArgT collectively regulate arginine availability towards intracellular *Salmonella* growth. *PLoS ONE* **5**, e15466.
- Datsenko, K. A. & Wanner, B. L. (2000). One-step inactivation of chromosomal genes in *Escherichia coli* K-12 using PCR products. *Proc Natl Acad Sci U S A* **97**, 6640–6645.
- Dieye, Y., Ameiss, K., Mellata, M. & Curtiss, R., III (2009). The *Salmonella* Pathogenicity Island (SPI) 1 contributes more than SPI2 to the colonization of the chicken by *Salmonella enterica* serovar Typhimurium. *BMC Microbiol* **9**, 3.
- Drecktrah, D., Levine-Wilkinson, S., Dam, T., Winfree, S., Knodler, L. A., Schroer, T. A. & Steele-Mortimer, O. (2008). Dynamic behavior of *Salmonella*-induced membrane tubules in epithelial cells. *Traffic* **9**, 2117–2129.
- Ehrbar, K., Friebel, A., Miller, S. I. & Hardt, W. D. (2003). Role of the *Salmonella* pathogenicity island 1 (SPI-1) protein InvB in type III secretion of SopE and SopE2, two *Salmonella* effector proteins encoded outside of SPI-1. *J Bacteriol* **185**, 6950–6967.
- Eisenreich, W., Dandekar, T., Heesemann, J. & Goebel, W. (2010). Carbon metabolism of intracellular bacterial pathogens and possible links to virulence. *Nat Rev Microbiol* **8**, 401–412.
- Eriksson, S., Lucchini, S., Thompson, A., Rhen, M. & Hinton, J. C. (2003). Unravelling the biology of macrophage infection by gene expression profiling of intracellular *Salmonella enterica*. *Mol Microbiol* **47**, 103–118.
- Eswarappa, S. M., Panguluri, K. K., Hensel, M. & Chakravorty, D. (2008). The *yejABEF* operon of *Salmonella* confers resistance to antimicrobial peptides and contributes to its virulence. *Microbiology* **154**, 666–678.
- Eswarappa, S. M., Karnam, G., Nagarajan, A. G., Chakraborty, S. & Chakravorty, D. (2009). *lac* repressor is an antivirulence factor of *Salmonella enterica*: its role in the evolution of virulence in *Salmonella*. *PLoS ONE* **4**, e5789.
- Ferguson, G. P. & Booth, I. R. (1998). Importance of glutathione for growth and survival of *Escherichia coli* cells: detoxification of methylglyoxal and maintenance of intracellular K<sup>+</sup>. *J Bacteriol* **180**, 4314–4318.
- Ferguson, G. P., McLaggan, D. & Booth, I. R. (1995). Potassium channel activation by glutathione-S-conjugates in *Escherichia coli*: protection against methylglyoxal is mediated by cytoplasmic acidification. *Mol Microbiol* **17**, 1025–1033.
- Ferguson, G. P., Nikolaev, Y., McLaggan, D., Maclean, M. & Booth, I. R. (1997). Survival during exposure to the electrophilic reagent N-ethylmaleimide in *Escherichia coli*: role of KefB and KefC potassium channels. *J Bacteriol* **179**, 1007–1012.
- Ferguson, G. P., Töttemeyer, S., MacLean, M. J. & Booth, I. R. (1998). Methylglyoxal production in bacteria: suicide or survival? *Arch Microbiol* **170**, 209–218.
- Fields, P. I., Swanson, R. V., Haidaris, C. G. & Heffron, F. (1986). Mutants of *Salmonella typhimurium* that cannot survive within the macrophage are avirulent. *Proc Natl Acad Sci U S A* **83**, 5189–5193.
- Ganz, T. (2003). Defensins: antimicrobial peptides of innate immunity. *Nat Rev Immunol* **3**, 710–720.
- Haneda, T., Ishii, Y., Danbara, H. & Okada, N. (2009). Genome-wide identification of novel genomic islands that contribute to *Salmonella* virulence in mouse systemic infection. *FEMS Microbiol Lett* **297**, 241–249.
- Haraga, A., Ohlson, M. B. & Miller, S. I. (2008). *Salmonellae* interplay with host cells. *Nat Rev Microbiol* **6**, 53–66.
- Hautefort, I., Thompson, A., Eriksson-Ygberg, S., Parker, M. L., Lucchini, S., Danino, V., Bongaerts, R. J. M., Ahmad, N., Rhen, M. & Hinton, J. C. (2008). During infection of epithelial cells *Salmonella*

- enterica* serovar Typhimurium undergoes a time-dependent transcriptional adaptation that results in simultaneous expression of three type 3 secretion systems. *Cell Microbiol* **10**, 958–984.
- Hölzer, S. U. & Hensel, M. (2010). Functional dissection of translocon proteins of the *Salmonella* pathogenicity island 2-encoded type III secretion system. *BMC Microbiol* **10**, 104.
- Hornef, M. W., Frisan, T., Vandewalle, A., Normark, S. & Richter-Dahlfors, A. (2002). Toll-like receptor 4 resides in the Golgi apparatus and colocalizes with internalized lipopolysaccharide in intestinal epithelial cells. *J Exp Med* **195**, 559–570.
- Jantsch, J., Chikkaballi, D. & Hensel, M. (2011). Cellular aspects of immunity to intracellular *Salmonella enterica*. *Immunol Rev* **240**, 185–195.
- Kim, J., Kim, O. S., Kim, C. S., Sohn, E., Jo, K. & Kim, J. S. (2012). Accumulation of argpyrimidine, a methylglyoxal-derived advanced glycation end product, increases apoptosis of lens epithelial cells both *in vitro* and *in vivo*. *Exp Mol Med* **44**, 167–175.
- Korithoski, B., Lévesque, C. M. & Cvitkovitch, D. G. (2007). Involvement of the detoxifying enzyme lactoylglutathione lyase in *Streptococcus mutans* aciduricity. *J Bacteriol* **189**, 7586–7592.
- Lara-Tejero, M. & Galán, J. E. (2009). *Salmonella enterica* serovar typhimurium pathogenicity island 1-encoded type III secretion system translocases mediate intimate attachment to nonphagocytic cells. *Infect Immun* **77**, 2635–2642.
- Loströh, C. P. & Lee, C. A. (2001). The *Salmonella* pathogenicity island-1 type III secretion system. *Microbes Infect* **3**, 1281–1291.
- Lucchini, S., Liu, H., Jin, Q., Hinton, J. C. & Yu, J. (2005). Transcriptional adaptation of *Shigella flexneri* during infection of macrophages and epithelial cells: insights into the strategies of a cytosolic bacterial pathogen. *Infect Immun* **73**, 88–102.
- MacLean, M. J., Ness, L. S., Ferguson, G. P. & Booth, I. R. (1998). The role of glyoxalase I in the detoxification of methylglyoxal and in the activation of the KefB K<sup>+</sup> efflux system in *Escherichia coli*. *Mol Microbiol* **27**, 563–571.
- Marathe, S. A., Ray, S. & Chakravorty, D. (2010). Curcumin increases the pathogenicity of *Salmonella enterica* serovar Typhimurium in murine model. *PLoS ONE* **5**, e11511.
- Marathe, S. A., Sen, M., Dasgupta, I. & Chakravorty, D. (2012). Differential modulation of intracellular survival of cytosolic and vacuolar pathogens by curcumin. *Antimicrob Agents Chemother* **56**, 5555–5567.
- Mercado-Lubo, R., Leatham, M. P., Conway, T. & Cohen, P. S. (2009). *Salmonella enterica* serovar Typhimurium mutants unable to convert malate to pyruvate and oxaloacetate are avirulent and immunogenic in BALB/c mice. *Infect Immun* **77**, 1397–1405.
- Nuding, S., Fellermann, K., Wehkamp, J., Mueller, H. A. & Stange, E. F. (2006). A flow cytometric assay to monitor antimicrobial activity of defensins and cationic tissue extracts. *J Microbiol Methods* **65**, 335–345.
- Ozyamak, E., Black, S. S., Walker, C. A., Maclean, M. J., Bartlett, W., Miller, S. & Booth, I. R. (2010). The critical role of S-lactoylglutathione formation during methylglyoxal detoxification in *Escherichia coli*. *Mol Microbiol* **78**, 1577–1590.
- Perrin, A. J., Jiang, X., Birmingham, C. L., So, N. S. & Brumell, J. H. (2004). Recognition of bacteria in the cytosol of mammalian cells by the ubiquitin system. *Curr Biol* **14**, 806–811.
- Pujol, C., Grabenstein, J. P., Perry, R. D. & Bliska, J. B. (2005). Replication of *Yersinia pestis* in interferon  $\gamma$ -activated macrophages requires *ripA*, a gene encoded in the pigmentation locus. *Proc Natl Acad Sci U S A* **102**, 12909–12914.
- Rachman, H., Kim, N., Ulrichs, T., Baumann, S., Pradl, L., Nasser Eddine, A., Bild, M., Rother, M., Kuban, R. J. & other authors (2006). Critical role of methylglyoxal and AGE in mycobacteria-induced macrophage apoptosis and activation. *PLoS ONE* **1**, e29.
- Rathman, M., Sjaastad, M. D. & Falkow, S. (1996). Acidification of phagosomes containing *Salmonella typhimurium* in murine macrophages. *Infect Immun* **64**, 2765–2773.
- Santiviago, C. A., Reynolds, M. M., Porwollik, S., Choi, S.-H., Long, F., Andrews-Polymeris, H. L. & McClelland, M. (2009). Analysis of pools of targeted *Salmonella* deletion mutants identifies novel genes affecting fitness during competitive infection in mice. *PLoS Pathog* **5**, e1000477.
- Sasikaran, J., Ziemski, M., Zadora, P. K., Fleig, A. & Berg, I. A. (2014). Bacterial itaconate degradation promotes pathogenicity. *Nat Chem Biol* **10**, 371–377.
- Shah, D. H., Lee, M. J., Park, J. H., Lee, J. H., Eo, S. K., Kwon, J. T. & Chae, J. S. (2005). Identification of *Salmonella gallinarum* virulence genes in a chicken infection model using PCR-based signature-tagged mutagenesis. *Microbiology* **151**, 3957–3968.
- Shi, L., Adkins, J. N., Coleman, J. R., Schepmoes, A. A., Dohnkova, A., Mottaz, H. M., Norbeck, A. D., Purvine, S. O., Manes, N. P. & other authors (2006). Proteomic analysis of *Salmonella enterica* serovar Typhimurium isolated from RAW 264.7 macrophages: identification of a novel protein that contributes to the replication of serovar Typhimurium inside macrophages. *J Biol Chem* **281**, 29131–29140.
- Steele-Mortimer, O. (2008). The *Salmonella*-containing vacuole: moving with the times. *Curr Opin Microbiol* **11**, 38–45.
- Thornalley, P. J. (2008). Protein and nucleotide damage by glyoxal and methylglyoxal in physiological systems – role in ageing and disease. *Drug Metabol Drug Interact* **23**, 125–150.
- Töttemeyer, S., Booth, N. A., Nichols, W. W., Dunbar, B. & Booth, I. R. (1998). From famine to feast: the role of methylglyoxal production in *Escherichia coli*. *Mol Microbiol* **27**, 553–562.
- Wong, D., Bach, H., Sun, J., Hmama, Z. & Av-Gay, Y. (2011). *Mycobacterium tuberculosis* protein tyrosine phosphatase (PtpA) excludes host vacuolar-H<sup>+</sup>-ATPase to inhibit phagosome acidification. *Proc Natl Acad Sci U S A* **108**, 19371–19376.
- Yadav, S. K., Singla-Pareek, S. L., Ray, M., Reddy, M. K. & Sopory, S. K. (2005). Methylglyoxal levels in plants under salinity stress are dependent on glyoxalase I and glutathione. *Biochem Biophys Res Commun* **337**, 61–67.
- Yu, X. J., McGourty, K., Liu, M., Unsworth, K. E. & Holden, D. W. (2010). pH sensing by intracellular *Salmonella* induces effector translocation. *Science* **328**, 1040–1043.

---

Edited by: D. Hood